

**NATIONAL CENTER FOR EARTHQUAKE
ENGINEERING RESEARCH**

State University of New York at Buffalo

**A Simulation Method for Stationary
Gaussian Random Functions
Based on the Sampling Theorem**

by

M. Grigoriu and S. Balopoulou

Department of Structural Engineering
School of Civil and Environmental Engineering
Cornell University
Ithaca, New York 14853

Technical Report NCEER-92-0015

June 11, 1992

This research was conducted at Cornell University and was partially supported by the National Science Foundation under Grant No. BCS 90-25010 and the New York State Science and Technology Foundation under Grant No. NEC-91029.

NOTICE

This report was prepared by Cornell University as a result of research sponsored by the National Center for Earthquake Engineering Research (NCEER) through grants from the National Science Foundation, the New York State Science and Technology Foundation, and other sponsors. Neither NCEER, associates of NCEER, its sponsors, Cornell University, nor any person acting on their behalf:

- a. makes any warranty, express or implied, with respect to the use of any information, apparatus, method, or process disclosed in this report or that such use may not infringe upon privately owned rights; or
- b. assumes any liabilities of whatsoever kind with respect to the use of, or the damage resulting from the use of, any information, apparatus, method or process disclosed in this report.

Any opinions, findings, and conclusions or recommendations expressed in this publication are those of the author(s) and do not necessarily reflect the views of NCEER, the National Science Foundation, the New York State Science and Technology Foundation, or other sponsors.

REPORT DOCUMENTATION PAGE	1. REPORT NO. NCEER-92-0015	2.	3. EB93-127496
4. Title and Subtitle A Simulation Method for Stationary Gaussian Random Functions Based on the Sampling Theorem		5. Report Date June 11, 1992	
7. Author(s) M. Grigoriu and S. Balopoulou		6.	
9. Performing Organization Name and Address Department of Structural Engineering School of Civil and Environmental Engineering Cornell University Ithaca, New York 14853		8. Performing Organization Rept. No.	
12. Sponsoring Organization Name and Address National Center for Earthquake Engineering Research State University of New York at Buffalo Red Jacket Quadrangle Buffalo, New York 14261		10. Project/Task/Work Unit No.	
15. Supplementary Notes This research was conducted at Cornell University and was partially supported by the National Science Foundation under Grant No. BCS 90-25010 and the New York State Science and Technology Foundation under Grant No. NEC-91029		11. Contract(C) or Grant(G) No. (C) BCS 90-25010 (G) NEC-91029	
16. Abstract (Limit: 200 words) A unified method is developed for simulating realizations of real-valued stationary Gaussian processes, vector processes, fields, and vector fields. The method has direct applications to earthquake engineering. Realizations of Gaussian processes and vector processes can be used to model seismic ground accelerations at single and multiple sites. Gaussian random fields can provide representations of the spatial variation of soil properties that need to be considered in earthquake engineering when dealing with systems extending over large areas such as pipeline systems. The proposed method in- volves parametric random models consisting of superpositions of deterministic functions of time or space with random fields. The proposed simulation method is efficient and uses algorithms for generating realizations of random processes and fields that are similar to simulation techniques based on ARMA models. Several examples are presented to demonstrate the proposed simulation method and evaluate its efficiency and accuracy.		13. Type of Report & Period Covered Technical Report	
17. Document Analysis a. Descriptors RANDOM PROCESSES. RANDOM FUNCTIONS. SAMPLING THEREOMS. RANDOM FIELDS. STATIONARY, GAUSSIAN PROCESSING. EARTHQUAKE ENGINEERING. b. Identifiers/Open-Ended Terms c. COSATI Field/Group		14.	
18. Availability Statement Release Unlimited		19. Security Class (This Report) Unclassified	21. No. of Pages 88
		20. Security Class (This Page) Unclassified	22. Price



**A Simulation Method for Stationary Gaussian Random
Functions Based on the Sampling Theorem**

by

M. Grigoriu¹ and S. Balopoulou²

June 11, 1992

Technical Report NCEER-92-0015

NCEER Project Numbers 90-1005 and 90-2002

NSF Master Contract Number BCS 90-25010

and

NYSSSTF Grant Number NEC-91029

- 1 Professor of Structural Engineering, School of Civil and Environmental Engineering, Cornell University
- 2 Graduate Research Assistant, School of Civil and Environmental Engineering, Cornell University

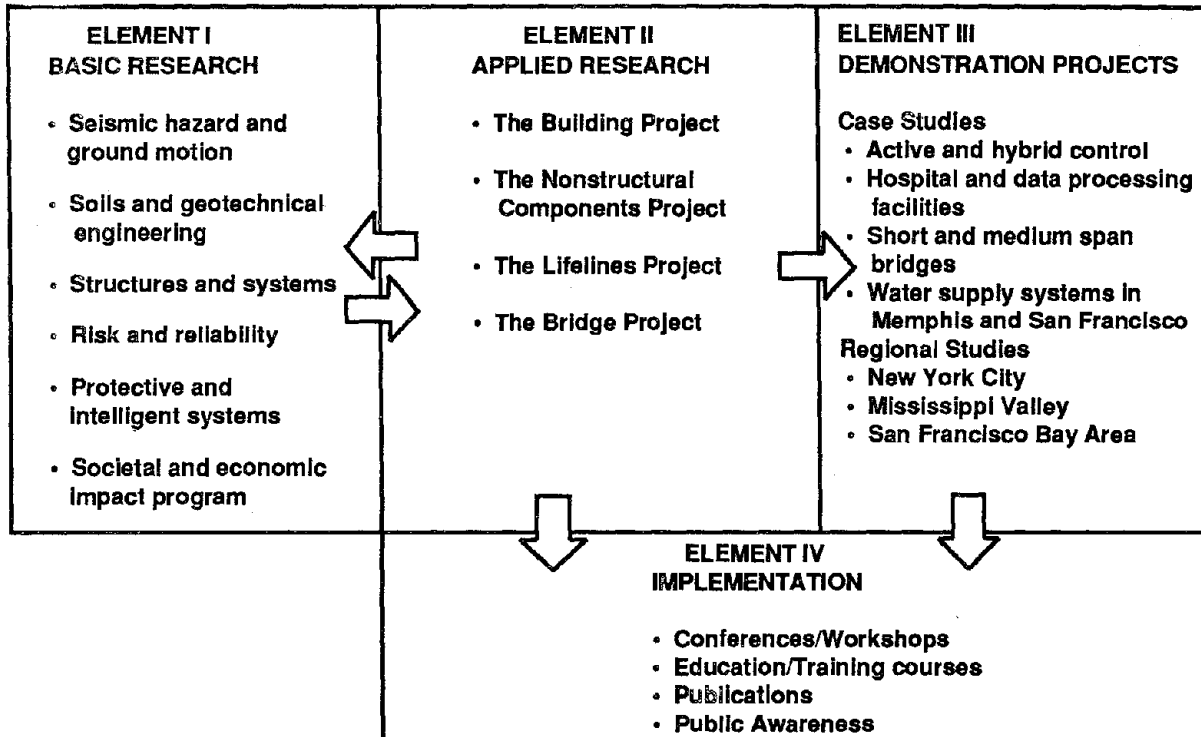
NATIONAL CENTER FOR EARTHQUAKE ENGINEERING RESEARCH
State University of New York at Buffalo
Red Jacket Quadrangle, Buffalo, NY 14261



PREFACE

The National Center for Earthquake Engineering Research (NCEER) was established to expand and disseminate knowledge about earthquakes, improve earthquake-resistant design, and implement seismic hazard mitigation procedures to minimize loss of lives and property. The emphasis is on structures in the eastern and central United States and lifelines throughout the country that are found in zones of low, moderate, and high seismicity.

NCEER's research and implementation plan in years six through ten (1991-1996) comprises four interlocked elements, as shown in the figure below. Element I, Basic Research, is carried out to support projects in the Applied Research area. Element II, Applied Research, is the major focus of work for years six through ten. Element III, Demonstration Projects, have been planned to support Applied Research projects, and will be either case studies or regional studies. Element IV, Implementation, will result from activity in the four Applied Research projects, and from Demonstration Projects.



Research in the **Building Project** focuses on the evaluation and retrofit of buildings in regions of moderate seismicity. Emphasis is on lightly reinforced concrete buildings, steel semi-rigid frames, and masonry walls or infills. The research involves small- and medium-scale shake table tests and full-scale component tests at several institutions. In a parallel effort, analytical models and computer programs are being developed to aid in the prediction of the response of these buildings to various types of ground motion.

Two of the short-term products of the **Building Project** will be a monograph on the evaluation of lightly reinforced concrete buildings and a state-of-the-art report on unreinforced masonry.

The **risk and reliability program** constitutes one of the important areas of research in the **Building Project**. The program is concerned with reducing the uncertainty in current models which characterize and predict seismically induced ground motion, and resulting structural damage and system unserviceability. The goal of the program is to provide analytical and empirical procedures to bridge the gap between traditional earthquake engineering and socioeconomic considerations for the most cost-effective seismic hazard mitigation. Among others, the following tasks are being carried out:

1. Study seismic damage and develop fragility curves for existing structures.
2. Develop retrofit and strengthening strategies.
3. Develop intelligent structures using high-tech and traditional sensors for on-line and real-time diagnoses of structural integrity under seismic excitation.
4. Improve and promote damage-control design for new structures.
5. Study critical code issues and assist code groups to upgrade seismic design code.
6. Investigate the integrity of nonstructural systems under seismic conditions.

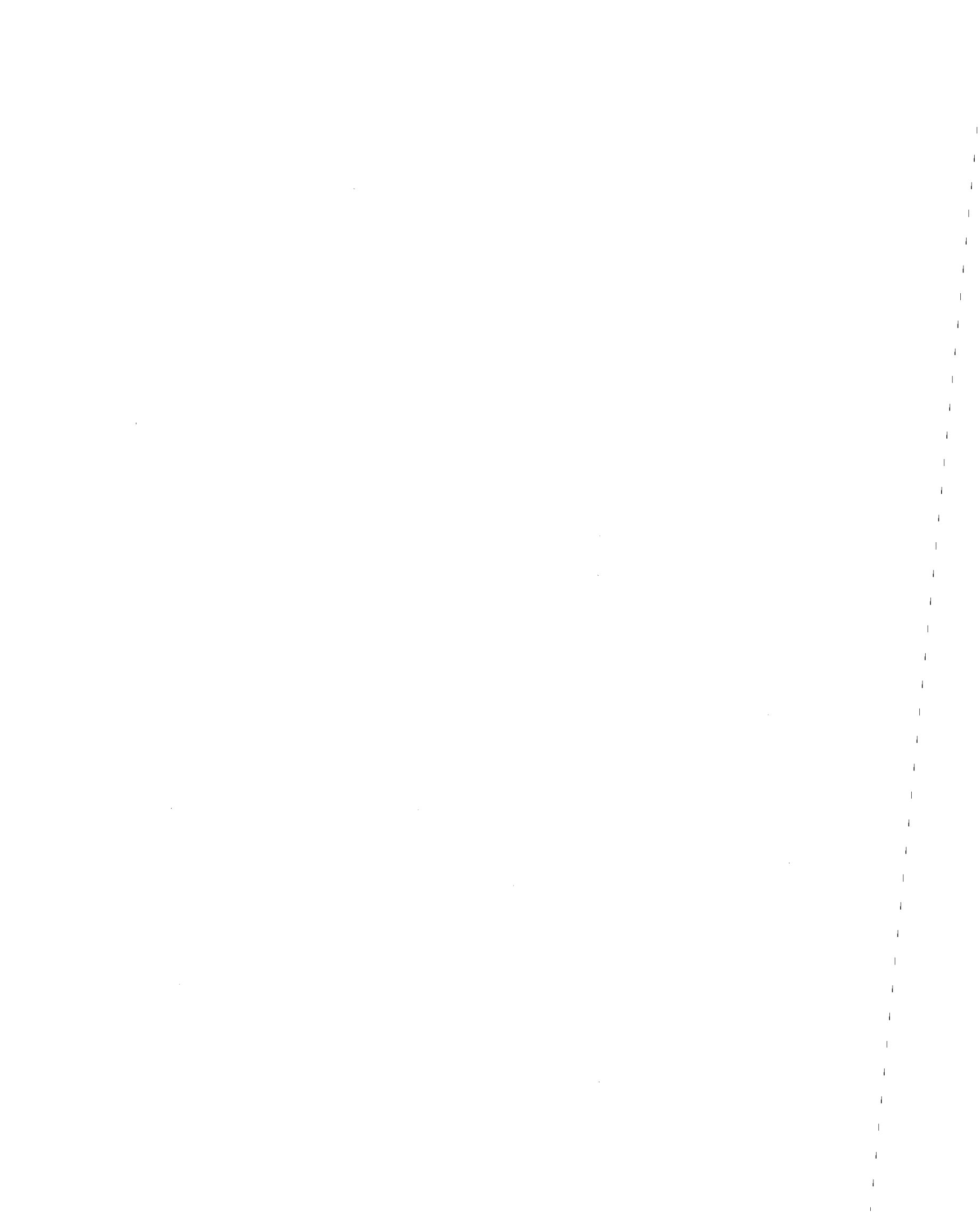
This report presents a new technique for simulating multidimensional and multivariate random processes. One version of the sampling theorem for deterministic functions is used as the starting point. The theorem is then extended from the deterministic case to the one-dimensional univariate random case, and then to the multidimensional, multivariate case. The global smoothing implicit in the sampling theorem is then replaced by a local smoothing which limits the size of the data required for simulating the random field at a given index location. The attraction of the new simulation technique is its limited storage requirement while sequentially simulating a random field in a manner analogous to the generation of ARMA processes. Asymptotic properties, as the smoothing window size tends to infinity, of the simulated random processes and fields is also discussed in the report. Several examples are presented that illustrate the proposed technique.

ABSTRACT

A unified method is developed for simulating realizations of real-valued stationary Gaussian processes, vector processes, fields, and vector fields. The method has direct applications to earthquake engineering. Realizations of Gaussian processes and vector processes can be used to model seismic ground accelerations at single and multiple sites. Gaussian random fields can provide representations of the spatial variation of soil properties that need to be considered in earthquake engineering when dealing with systems extending over large areas such as pipeline systems. The proposed method involves parametric random models consisting of superpositions of deterministic functions of time or space with random amplitudes. The parametric models are based on the sampling theorem for random processes and generalizations of it for vector processes and random fields. The proposed simulation method is efficient and uses algorithms for generating realizations of random processes and fields that are similar to simulation techniques based on ARMA models. Several examples are presented to demonstrate the proposed simulation method and evaluate its efficiency and accuracy.

TABLE OF CONTENTS

SECTION	TITLE	PAGE
1	INTRODUCTION	1-1
2	SAMPLING THEOREM FOR DETERMINISTIC FUNCTIONS	2-1
2.1	Sampling Theorem ($q = 1, p = 1$)	2-1
2.2.	Generalized Sampling Theorem ($q > 1$ and/or $p > 1$)	2-1
3	SAMPLING THEOREM FOR RANDOM FUNCTIONS	3-1
3.1	Random Processes ($q = 1, p = 1$)	3-1
3.1.1.	Narrow-Band Random Processes	3-5
3.1.2.	Local Representation of $X(t)$	3-8
3.2	Vector Random Processes ($q = 1, p > 1$)	3-10
3.3	Random Fields ($q > 1, p = 1$)	3-14
3.4	Vector Random Fields ($q > 1, p > 1$)	3-18
4	SIMULATION ALGORITHMS	4-1
4.1	Random Processes ($q = 1, p = 1$)	4-1
4.2	Vector Random Processes ($q = 1, p > 1$)	4-10
4.3	Random Fields ($q > 1, p = 1$)	4-21
5	CONCLUSIONS	5-1
6	REFERENCES	6-1
	APPENDIX	A-1



LIST OF ILLUSTRATIONS

FIGURE	TITLE	PAGE
4-1	Covariance Functions of $Y_n(t)$ in Eq. (3.19) and $X(t)$ for a Band-Limited White Noise Process	4-3
4-2	Histograms of $Y_n(t)$ in Eq. (3.19) for Band-Limited White Noise and Truncated First Order Gauss-Markov Processes	4-4
4-3	Mean Upcrossing Rates for Band-Limited White Noise, Truncated First Order Gauss-Markov, and Envelope of a Narrow Band Gaussian Process with Constant Power within a Small Frequency Range	4-7
4-4	Covariance Functions of $\underline{Y}_n(t)$ in Eq. (3.30) and $\underline{X}(t)$ for the Bivariate Gaussian Process $\underline{X}(t)$ in Eq. (4.8) with $\rho = 0.5$	4-14
4-5	Covariance functions of $\underline{Y}_n(t)$ in Eq. (3.30) and $\underline{X}(t)$ for the bivariate Gaussian Process $\underline{X}(t)$ in Eq. (4.14)	4-18
4-6	Domain $D = [0, a_1] \times [0, a_2] = [0, \bar{n}_1 T_1] \times [0, \bar{n}_2 T_2]$, Partition in Cells, Cell Numbers, and Nodal Points	4-22
4-7	Covariance Functions of $Y_n(\underline{t})$ in Eq. (3.36) and $X(\underline{t})$ for a Bivariate Band-Limited Gaussian White Noise Random Field	4-25
4-8	Covariance Functions of $Y_n(\underline{t})$ in Eq. (3.36) and $X(\underline{t})$ for a Bivariate Random Field with Truncated Gaussian Spectrum	4-28

LIST OF TABLES

TABLE	TITLE	PAGE
4-I	Estimated Variances of $Y_n(t)$ for a Band-Limited White Noise	4-5
4-II	Estimated Variances for a Truncated First Order Gauss-Markov Process	4-6
4-III	Mean Upcrossings Rates for a Band-Limited Gaussian White Noise Process	4-8
4-IV	Mean Upcrossing Rates for a Truncated First Order Gauss-Markov Process	4-8
4-V	Mean Upcrossing Rates of the Envelope of a Narrow Band Gaussian Process	4-9
4-VI	Mean D-Outcrossing Rates of $\underline{X}(t)$	4-16

SECTION 1 INTRODUCTION

Continuous and discrete time models are currently used to generate realizations of a stationary Gaussian stochastic process. The continuous models generally consist of a finite sum of harmonics with random phase and deterministic or random amplitude [13,15]. They can be obtained by approximating the power spectral density of the process by a discrete spectrum with power at a finite number of frequencies. These models are simple and can be applied to generate Gaussian processes and fields [12,13,14,15]. However, the computer storage required for generation can be excessive. The autoregressive moving average (ARMA) random sequences are the most common discrete time models that are used in simulation [5,8,10,16]. The main feature of the ARMA models is that the sample generation can be performed on-line such that the computer storage demand is minimum. On the other hand, the calibration of these models to a target stochastic process can be complex. Moreover, the ARMA models have only been applied to generate samples of random processes.

Current simulation algorithms based on continuous and discrete time models can be extended to generate realizations of a class of non-Gaussian random functions that can be obtained from Gaussian processes by memoryless transformations [6,19]. The continuous and discrete time models can also be generalized to represent nonstationary processes by, e.g., modulating the amplitude or the amplitude and phase of a stationary process [7,11], considering ARMA models with time-dependent coefficients [5], or using the Priestley process with evolutionary spectrum [7,11].

This report presents a unified method for simulating realizations of stationary Gaussian processes, vector processes, fields, and vector fields

that has direct applications to earthquake engineering. Realizations of Gaussian processes and vector processes can be used to represent the seismic ground acceleration at single and multiple sites. Gaussian random fields can provide models of the spatial variation of soil properties that need to be considered in earthquake engineering when dealing with systems extending over large areas such as pipeline systems.

The method is based on parametric random functions depending on a finite number of dependent Gaussian variables. The parametric models in the report can be obtained from the sampling theorem. The proposed method has attractive features. It is simple, efficient, and allows on-line simulation as the ARMA model. Moreover, the accuracy of the model can be calculated prior to simulation. The algorithm for generating realizations of a Gaussian random function is less simple because of minor bookkeeping problems and the need to generate dependent Gaussian random variables. However, these are not significant inconveniences because the simulation algorithm needs to be codified once and efficient algorithms are available for generating dependent Gaussian variables [9].

SECTION 2
SAMPLING THEOREM FOR DETERMINISTIC FUNCTIONS

Consider a deterministic function g defined on R^q , $q = 1, 2, \dots$, with values in R^p , $p = 1, 2, \dots$. It is assumed that the components $g_r(\underline{t})$, $r = 1, 2, \dots, p$, of $g(\underline{t})$ have band-limited Fourier transforms in the frequency range $(-\bar{f}_{rs}, \bar{f}_{rs})$, $0 < \bar{f}_{rs} < \infty$, $r = 1, \dots, p$, $s = 1, \dots, q$.

2.1 Sampling Theorem ($q = 1$, $p = 1$)

Suppose that function g is real-valued and defined on the real line R . Let $\bar{f} = \bar{f}_{11}$ be the band-width of the function. According to the sampling theorem [2,18]

$$g(t) = \sum_{k=-\infty}^{\infty} g(t_0 + kT) \alpha_k(t - t_0; T) \quad (2.1)$$

in which

$$\alpha_k(u; T) = \frac{\sin [\pi(u - kT)/T]}{\pi(u - kT)/T} \quad (2.2)$$

$T = 1/(2\bar{f})$, and t_0 any real number.

2.2 Generalized Sampling Theorem ($q > 1$ and/or $p > 1$)

Three cases are examined: (1) $q = 1$, $p > 1$; (2) $q > 1$, $p = 1$; and (3) $p > 1$, $q > 1$. They correspond to a vector function $g(t)$; real-valued function $g(\underline{t})$ defined in R^q ; and vector function $g(\underline{t})$ defined on R^q with values on R^p .

Case 1 ($q = 1$, $p > 1$): Let $g_r(t)$, $r = 1, \dots, p$, be the components of $g(t)$ that are assumed to have a finite bandwidth with power concentrated in the

frequency range $(-\bar{f}_r, \bar{f}_r)$, where $\bar{f}_r = \bar{f}_{r1}$. The sampling theorem in Eqs. (2.1) and (2.2) applies to every component $g_r(t)$ of $g(t)$ so that

$$g_r(t) = \sum_{k=-\infty}^{\infty} g_r(t_{r,0} + kT_r) \alpha_k(t-t_{r,0}; T_r) \quad (2.3)$$

in which $T_r = 1/(2\bar{f}_r)$ and $t_{r,0}$ is an arbitrary real number.

Case 2 ($q > 1, p = 1$). Suppose that the Fourier transform of function $g: \mathbb{R}^q \rightarrow \mathbb{R}$ exists and vanishes outside a set $A = \prod_{s=1}^q (-\bar{f}_s, \bar{f}_s)$, where $\bar{f}_s = \bar{f}_{1s}$, $s = 1, \dots, q$. Then, function g can be represented by the series expansion

$$g(\underline{t}) = \sum_{k_1=-\infty}^{\infty} \dots \sum_{k_q=-\infty}^{\infty} g(t_{1,0} + k_1 T_1, \dots, t_{q,0} + k_q T_q) \prod_{s=1}^q \alpha_{k_s}(t_s - t_{s,0}; T_s) \quad (2.4)$$

where $T_s = 1/(2\bar{f}_s)$ and $\{t_{s,0}\}$ are arbitrary real numbers, $s = 1, \dots, q$.

The result follows from the sampling theorem. Suppose that (t_2, \dots, t_q) are fixed. According to Eqs. (2.1) and (2.2),

$$g(\underline{t}) = \sum_{k_1=-\infty}^{\infty} g(t_{1,0} + k_1 T_1, t_2, \dots, t_q) \alpha_{k_1}(t_1 - t_{1,0}; T_1) \quad (2.5)$$

Using similar considerations for all arguments of $g(\underline{t})$ one finds the result in Eq. (2.4).

Case 3 ($q > 1, p > 1$). Let $g_r(\underline{t})$, $r = 1, \dots, p$, be the real-valued functions defining the vector function $g(\underline{t})$. The components $g_r(\underline{t})$ of $g(\underline{t})$ satisfy the conditions in the previous case such that Eq. (2.4) applies and

$$g_r(\underline{t}) = \sum_{k_1=-\infty}^{\infty} \cdots \sum_{k_q=-\infty}^{\infty} g_r(t_{r1,0} + k_1 T_{r1}, \dots, t_{rq,0} + k_q T_{rq})$$

$$* \prod_{s=1}^q \alpha_{k_s}(t_s - t_{rs,0}; T_{si}), \quad r = 1, \dots, p \quad (2.6)$$

in which $T_{rs} = 1/(2f_{rs})$ and $t_{rs,0}$ are arbitrary real numbers.

SECTION 3
SAMPLING THEOREM FOR RANDOM FUNCTIONS

Consider a zero-mean stationary Gaussian function $\underline{X}(\underline{t})$ defined on R^q with values on R^p , $p, q = 1, 2, \dots$. It has the covariance functions

$$c_{ru}(\underline{\tau}) = EX_r(\underline{t} + \underline{\tau}) X_u(\underline{t}) \quad , \quad r, u = 1, 2, \dots, p \quad (3.1)$$

and mean power spectral densities

$$s_{ru}(\underline{f}) = \int_{R^q} e^{-i2\pi\underline{f}'\underline{\tau}} c_{ru}(\underline{\tau}) d\underline{\tau} \quad (3.2)$$

in which $i = \sqrt{-1}$ and the symbol $'$ denotes vector and matrix transposition. It is assumed that the mean power spectral densities of the components $X_r(\underline{t})$, $r = 1, \dots, p$, of $\underline{X}(\underline{t})$ are concentrated on the intervals $\prod_{s=1}^q (-\bar{f}_{rs}, \bar{f}_{rs})$, $0 < \bar{f}_{rs} < \infty$, $r = 1, \dots, p$, $s = 1, \dots, q$.

3.1 Random Processes ($q = 1, p = 1$)

The real-valued zero-mean stationary process $X(t)$, $t \in R$, has covariance function $c(\tau) = E X(t+\tau) X(t)$ and a power spectral density $s(f) = \int_R e^{-i2\pi f\tau} c(\tau) d\tau$ vanishing outside a bounded interval $(-\bar{f}, \bar{f})$, $0 < \bar{f} < \infty$.

From the sampling theorem in Eq. (2.1) with $T = 1/2\bar{f}$

$$c(\tau) = \sum_{k=-\infty}^{\infty} c(\tau_0 + kT) \alpha_k(\tau - \tau_0; T) \quad (3.3)$$

for any real τ_0 because $c(\tau)$ is a deterministic function whose Fourier transform coincides with the spectral density $s(f)$ that is concentrated on $(-\bar{f}, \bar{f})$, $0 < \bar{f} < \infty$.

Define the family of parametric stochastic processes

$$X_N(t) = \sum_{k=-N}^N X_k \alpha_k(t; T) \quad (3.4)$$

in which $N = 1, 2, \dots$ and $X_k = X(kT)$ are random variables that are fully defined by the finite dimensional distributions of $X(t)$. The instances kT , $k = -N, \dots, N$ are called the nodal points. The parametric processes $X_N(t)$ have several interesting properties that suggest their use as approximations of $X(t)$.

Proposition 1. $X_N(t)$ in Eq. (3.4) has the same first two moments as $X(t)$ asymptotically as $N \rightarrow \infty$ [18].

The mean of $X_N(t)$ is zero for any value of N because $EX_k = EX(kT) = 0$, $k = -N, \dots, N$. The cross-covariance of the two parametric representations of order N and M is

$$\begin{aligned} c_{N,M}(t+r, t) &= E X_N(t+r) X_M(t) \\ &= \sum_{k=-N}^N \alpha_k(t+r; T) \sum_{\ell=-M}^M c((k-\ell)T) \alpha_\ell(t; T) \end{aligned} \quad (3.5)$$

Denote by

$$h_k(t; M) = \sum_{\ell=-M}^M c((k-\ell)T) \alpha_\ell(t; T) - \sum_{\ell=-M}^M c(-kT+\ell T) \alpha_\ell((t-kT) + kT; T) \quad (3.6)$$

the second sum after index ℓ in Eq. (3.5) and let M approach infinity. From Eq. (3.3), $h_k(t; M)$ converges to $c(t-kT)$ as $M \rightarrow \infty$. Using again Eq. (3.3) it

can be shown that the remaining sum in Eq. (3.5) after index k , approaches $c(\tau)$ as $N \rightarrow \infty$.

The covariance function in Eq. (3.5) shows that the family of processes $X_N(t)$ with $N < \infty$ is not stationary in the wide sense. This is caused by the dependence of $X_N(t)$ on a finite number of values of $X(t)$ in the bounded range $(-NT, NT)$ when $N < \infty$. According to Proposition 1, $X_N(t)$ approaches stationarity in the wide sense as $N \rightarrow \infty$.

The Proposition also shows that $X_N(t)$ provides a satisfactory approximation of $X(t)$ for large values of N . The approximation does not hold when t is close to the boundary of the interval $(-NT, NT)$ or outside it. In fact, $X_N(t)$ for $N < \infty$ approaches zero as t increases indefinitely because the functions $\alpha_k(t; T)$ in the representation of the process vanish as $t \rightarrow \infty$. This problem can be eliminated by letting N increase indefinitely. However, the resultant model $X_N(t)$ would become impractical for simulation. An alternative local representation of $X(t)$ is proposed in Sec. 3.1.2 for efficient simulation.

Proposition 2 (Sampling Theorem). $X_N(t)$ in Eq. (3.4) approaches $X(t)$ in the mean square sense as $N \rightarrow \infty$, i.e.,

$$\lim_{N \rightarrow \infty} E(X_N(t) - X(t))^2 = 0 \quad (3.7)$$

The proof of this statement is similar to that of Proposition 1 and can be found in textbooks [18].

Let

$$\Delta_N(t) = X(t) - X_N(t) \quad (3.8)$$

be the error of the approximation $X_N(t)$ of $X(t)$. The difference $\Delta_N(t)$ is a zero-mean random process with variance

$$E \Delta_N(t)^2 = \sum_{|k|, |\ell| > N} c((k-\ell)T) \alpha_k(t; T) \alpha_\ell(t; T) \quad (3.9)$$

The variance of this error process $\Delta_N(t)$ depends on t and provides useful information on the order of the approximation required in the analysis. For example, let t be a multiple of T . Then, $E\Delta_N(t)^2$ is equal to zero or one when $|t| \leq N$ or $|t| > N$. Therefore, errors can be significant if $X(t)$ is approximated by $X_N(t)$ and $|t| > N$.

Proposition 3. Suppose that the process $X(t)$ in the previous two propositions is Gaussian. Then, $X_N(t)$ in Eq. (3.4) is a version of $X(t)$ asymptotically as $N \rightarrow \infty$.

From Proposition 1, $X_N(t)$ is equal to $X(t)$ in the second-moment sense asymptotically as $N \rightarrow \infty$. From Eq. (3.4) and the hypothesis that $X(t)$ is Gaussian, the parametric representations $X_N(t)$ are Gaussian processes for any value of N as linear combinations of the Gaussian variables $\{X_k\}$. Therefore, all finite dimensional distributions of $X(t)$ and $X_N(t)$ coincide asymptotically as $N \rightarrow \infty$ because they only depend on the mean and covariance functions of these processes.

There is no simple extension of the statement in Proposition 3 to the case of non-Gaussian processes. When $X(t)$ is not Gaussian the finite dimensional distributions of any order of $X(t)$ and $X_N(t)$ coincide provided that (i) the instances $\{t_i\}$ at which these distributions are calculated coincide with nodal points and (ii) N is sufficiently large such that $t_i \in (-NT, NT)$ for all indices i . The coincidence of these distributions follows from Eq. (3.4)

showing that $X_N(t_i) = X(t_i)$ when t_i is a multiple of T and belongs to $(-NT, NT)$. The distribution of $X_N(t)$ at instances different from nodal points can be calculated but its determination is complex.

3.1.1. Narrow-Band Random Processes ($q = 1, p = 1$)

Suppose that the zero-mean, stationary, band-limited process $X(t)$ has a power spectral density $s(f)$ that is zero outside the set $(-\bar{f} - f_0, -f_0 + \bar{f}) \cup (-\bar{f} + f_0, f_0 + \bar{f})$ in which $0 < \bar{f} \ll f_0 < \infty$. The power of the process is concentrated in small vicinities centered on the frequencies $\pm f_0$. Results of Propositions 1-3 and the parametric representation in Eq. 3.4 are still valid. However, the representation is impractical because the required sampling $1/(2f_0)$ can be very dense when f_0 is large.

An alternative parametric representation can be used for narrow-band processes. The representation is based on a classical definition of narrow band processes [3,4],

$$X(t) = V(t) \cos(2\pi f_0 t + \psi(t)) \quad (3.10)$$

and

$$X(t) = X_c(t) \cos(2\pi f_0 t) + X_s(t) \sin(2\pi f_0 t) \quad (3.11)$$

in which

$$V(t) = (X_c(t)^2 + X_s(t)^2)^{1/2} \quad (3.12)$$

$$\psi(t) = \tan^{-1} \left[-\frac{X_s(t)}{X_c(t)} \right]$$

Processes $X_c(t)$ and $X_s(t)$ are linear transformations of $X(t)$ such that their mean is zero, are stationary, and have the covariance functions

$$\begin{aligned}\tilde{c}(\tau) &= E X_c(t+\tau) X_c(t) = E X_s(t+\tau) X_s(t) \\ &= 4\pi \int_{-\tilde{f}}^{\tilde{f}} d\nu s(\nu+f_0) \cos(2\pi\nu\tau)\end{aligned}\quad (3.13)$$

and

$$\begin{aligned}\hat{c}(\tau) &= E X_c(t+\tau) X_s(t) = -E X_c(t) X_s(t+\tau) \\ &= 4\pi \int_{-\tilde{f}}^{\tilde{f}} d\nu s(\nu+f_0) \sin(2\pi\nu\tau)\end{aligned}\quad (3.14)$$

These processes are uncorrelated when the spectrum $s(f)$ is symmetric about the central frequency f_0 because $\hat{c}(\tau)$ is zero for all values of τ . The random variables $X_c(t)$ and $X_s(t)$ are uncorrelated for any value of t irrespective of the shape of $s(f)$.

Consider the parametric family of stochastic processes

$$X_N(t) = X_{N,c}(t) \cos(2\pi f_0 t) + X_{N,s}(t) \sin(2\pi f_0 t) \quad (3.15)$$

in which

$$\begin{aligned}X_{N,c}(t) &= \sum_{k=-N}^N X_{c,k} \alpha_k(t; T) \\ X_{N,s}(t) &= \sum_{k=-N}^N X_{s,k} \alpha_k(t; T)\end{aligned}\quad (3.16)$$

$X_{c,k} = X_c(kT)$, $X_{s,k} = X_s(kT)$, and α_k ; T are defined in Eq. (3.4). Processes $X_{N,c}(t)$ and $X_{N,s}(t)$ are Gaussian as linear combinations of discrete values of $X_c(t)$ and $X_s(t)$ and are fully defined by the probability of these processes. The sampling rate, $T = 1/2f$, used to define processes $X_{N,c}(t)$ and $X_{N,s}(t)$ is much lower than the required sampling rate, $1/2(f_0 + \bar{f})$, corresponding to a direct use of Eq. (3.4) for process $X(t)$.

Proposition 4. $X_N(t)$ in Eqs. (3.14) and (3.16) has the same first two moments as $X(t)$ asymptotically as $N \rightarrow \infty$.

The mean of $X_N(t)$ is zero for any value of N because $X_c(t)$ and $X_s(t)$ are linear transformations of $X(t)$. The covariance function of two parametric representations of order N and M is

$$\begin{aligned}
 c_{N,M}(t+\tau, t) &= E X_N(t+\tau) X_M(t) \\
 &= \sum_{k=-N}^N \alpha_k(t+\tau) \sum_{\ell=-M}^M \tilde{c}((k-\ell)T) \alpha_\ell(t) \cos(2\pi f_0 \tau) \\
 &\quad - \sum_{k=-N}^N \alpha_k(t+\tau) \sum_{\ell=-M}^M \hat{c}((k-\ell)T) \alpha_\ell(t) \sin(2\pi f_0 \tau) \quad (3.17)
 \end{aligned}$$

Using arguments as in Eqs. (3.5) and (3.6) it can be shown that

$$\lim_{\substack{N \rightarrow \infty \\ M \rightarrow \infty}} c_{N,M}(t+\tau, t) = \tilde{c}(\tau) \cos(2\pi f_0 \tau) - \hat{c}(\tau) \sin(2\pi f_0 \tau) \quad (3.18)$$

The limit coincides with the covariance $c(\tau)$ of $X(t)$ as it can be found by direct calculations.

Results in Propositions 2 and 3 can also be extended directly to narrow-band processes [11]. Thus, $X_N(t)$ in Eqs. (3.15) and (3.16) approaches $X(t)$ in the mean square sense as $N \rightarrow \infty$. Moreover, $X_N(t)$ is a version of $X(t)$ asymptotically as $N \rightarrow \infty$ provided that $X(t)$ is Gaussian. In this case the parametric processes $X_N(t)$ are Gaussian for any value of N as linear transformations of values of $X(t)$ at the nodal points.

3.1.2 Local Representation of $X(t)$

Consider a band-limited, zero-mean stationary Gaussian process that can be approximated by $X_N(t)$ in Eq. (3.4). An alternative representation of $X(t)$ is

$$Y_n(t) = \sum_{k=n_t-n}^{n_t+n+1} X_k \alpha_k(t; T) \quad , \quad n_t T \leq t \leq (n_t+1)T \quad (3.19)$$

in which $n_t = [t/T]$ - the largest integer smaller than t/T and n is a positive integer. The representation has a local character because it involves $2(n+1)$ nodal values of $X(t)$ centered about the active cell $[n_t T, (n_t+1)T]$, i.e., the cell containing current time t . The choice of n defines the size of the window or vicinity about the active cell.

The local representation in Eq. (3.19) has similar asymptotic properties as $X_N(t)$ in Eq. (3.4). For example, it can be shown that $Y_n(t)$ has the same mean and covariance function as $X(t)$ asymptotically as $n \rightarrow \infty$. Moreover, the process $Y_n(t)$ is a version of $X(t)$ as $n \rightarrow \infty$ when $X(t)$ is a Gaussian process.

There is a notable difference between the representations in Eqs. (3.4) and (3.19). Although they both involve values of $X(t)$ equally spaced at

$T = 1/(2f)$, these values are centered about zero for $X_N(t)$ and about t for $Y_n(t)$. As t increases N must take large values to assure that t is included in $(-NT, NT)$ and $X_N(t)$ provides an accurate approximation of $X(t)$. On the other hand, the representation $Y_n(t)$ involves $2(n+1)$ values of $X(t)$ at any time t . This feature is particularly attractive in simulation because the generation of samples of $Y_n(t)$ depends on a relatively small number of random variables that can be generated sequentially as time t increases. In contrast, simulation based on $X_N(t)$ requires to generate samples of all variables $\{X_k\}$, $k = -N, \dots, N$ and store their values prior to the determination of a realization of $X_N(t)$.

The local representation in Eq. (3.19) can be extended without difficulties to the case in which $X(t)$ is a narrow-band stationary Gaussian process with power centered at the frequencies $\pm f_0$. A global approximation of the process is $X_N(t)$ in Eqs. (3.15) and (3.16). A local approximation of the process can be provided by the model

$$Y_n(t) = Y_{n,c}(t) \cos(2\pi f_0 t) + Y_{n,s}(t) \sin(2\pi f_0 t), \quad n_t T \leq t \leq (n_t + 1)T \quad (3.20)$$

in which

$$Y_{n,c}(t) = \sum_{k=n_t-n}^{n_t+n+1} X_{c,k} \alpha_k(t; T) \quad (3.21)$$

$$Y_{n,s}(t) = \sum_{k=n_t-n}^{n_t+n+1} X_{s,k} \alpha_k(t; T)$$

with n_t and n as in Eq. (3.19). The local representation $Y_n(t)$ of $X(t)$ has the same asymptotic properties as $X_N(t)$ in Eqs. (3.15) and (3.16). The

representation is more suitable for simulation since, as $Y_n(t)$ in Eq. (3.19), involves a smaller number of random variables that can be generated sequentially. Moreover, the number of random variables in the representation $Y_n(t)$ of $X(t)$ is independent of t . It only depends on the size n of the window considered in the representation.

The local representations in Eqs. (3.19) and (3.20) have continuous samples. However, they are not differentiable at the nodal points. For example, the discrepancy between the right and left derivatives of $Y_n(t)$ in Eq. (3.19) at a nodal point $n_t T$ is

$$\dot{Y}_n(n_t T+) - \dot{Y}_n(n_t T-) = X((n_t+n+1)T) \dot{\alpha}_{n_t+n+1}(n_t T; T) - X((n_t-n-1)T) \dot{\alpha}_{n_t-n-1}(n_t T; T) \quad (3.22)$$

This difference decreases with n and vanishes asymptotically as $n \rightarrow \infty$.

3.2 Vector Random Processes ($q = 1, p > 1$)

Consider a zero-mean stationary Gaussian vector process $\underline{X}(t)$ with components $X_r(t)$, $r = 1, \dots, p$. The Gaussian process $X_r(t)$ have mean zero, bandwidth $(-\bar{f}_r, \bar{f}_r)$, $\bar{f}_r = \bar{f}_{r1}$, $0 < \bar{f}_r < \infty$, covariance function $c_{ru}(\tau) = E X_r(t+\tau) X_u(t)$ and mean power spectral densities $s_{ru}(f) = \int_{-\infty}^{\infty} e^{-i2\pi f\tau} c_{ru}(\tau) d\tau$, $r, u = 1, \dots, p$. Let

$$X_{r, N_r}(t) = \sum_{k=-N_r}^{N_r} X_{r, k} \alpha_k(t; T_r) \quad (3.23)$$

be parametric representations of the process $X_r(t)$, in which $X_{r, k} = X_r(kT_r)$, $T_r = 1/(2\bar{f}_r)$, and α_k is defined in Eq. 2.2. Let

$$\underline{X}_{\underline{N}}(t) = \begin{bmatrix} X_{1, N_1}(t) \\ \vdots \\ X_{p, N_p}(t) \end{bmatrix} \quad (3.24)$$

be a vector of parametric random process of order $\underline{N} = (N_1, \dots, N_p)'$.

Proposition 5. Process $X_{r, N_r}(t)$ has the same first two moments as $X_r(t)$ asymptotically as $N_r \rightarrow \infty$, $r = 1, \dots, p$. Moreover, $X_{r, N_r}(t)$ approaches $X_r(t)$ in the mean square sense as $N_r \rightarrow \infty$, $r = 1, \dots, p$.

The proof follows from Propositions 1 and 2.

Proposition 6. The vector process $\underline{X}_{\underline{N}}(t)$ approaches $\underline{X}(t)$ in the mean square sense as $N_r \rightarrow \infty$, $r = 1, \dots, p$.

It is needed to show that the processes $\underline{X}(t)$ and $\underline{X}_{\underline{N}}(t)$ have the same mean and covariance functions as $N_r \rightarrow \infty$, $r = 1, \dots, p$. The mean of $\underline{X}_{\underline{N}}(t)$ is zero for any values of N_r , $r = 1, \dots, p$ because $E X_{r, k} = 0$ for all k and r by hypothesis. Consider the covariance function of two arbitrary components of $\underline{X}_{\underline{N}}(t)$. This covariance is

$$\begin{aligned} c_{N_r, N_u}(t+r, t) &= E X_{N_r}(t+r) X_{N_u}(t) \\ &= \sum_{\xi=-N_r}^{N_r} \sum_{\xi=-N_u}^{N_u} c_{ru}(\xi T_r - \xi T_u) \alpha_{\xi}(t+r, T_r) \alpha_{\xi}(t; T_u) \\ &= \sum_{\xi=-N_r}^{N_r} \alpha_{\xi}(t+r; T_r) g_{ru, N_u}(t; T_r, T_u) \end{aligned} \quad (3.25)$$

in which

$$g_{ru, N_u}(t; T_r, T_u) = \sum_{\xi=-N_u}^{N_u} c_{ru}(\xi T_r - \xi T_u) \alpha_{\xi}(t; T_u) \quad (3.26)$$

or

$$g_{ru, N_u}(t; T_r, T_u) = \sum_{\xi=-N_u}^{N_u} c_{ur}(\xi T_u + \tau_0) \alpha_{\xi}(t' - \tau_0; T_u) \quad (3.27)$$

with $\tau_0 = -u T_r$ and $t' = t + \tau_0$ because $c_{ru}(\tau) = c_{ur}(-\tau)$. From Eq. (3.26) $g_{ru, N_u}(t; T_r, T_u)$ approaches $c_{ur}(t') = c_{ur}(t - uT_k)$ as $N_u \rightarrow \infty$. The limit for $N_r \rightarrow \infty$ in Eq. (3.26) gives

$$\begin{aligned} \lim_{\substack{N_r \rightarrow \infty \\ N_u \rightarrow \infty}} c_{N_r, N_u}(t+\tau, t) &= \lim_{N_r \rightarrow \infty} \sum_{\zeta=-N_r}^{N_r} c_{ur}(t - \zeta T_r) \alpha_{\zeta}(t+\tau; T_r) \\ &= \lim_{N_r \rightarrow \infty} \sum_{\zeta=-N_r}^{N_r} c_{ru}(\zeta T_r - t) \alpha_{\zeta}(t+\tau; T_r) \end{aligned} \quad (3.28)$$

and is equal to $c_{ru}(\tau)$ because

$$c_{ru}(\tau) = \sum_{k=-\infty}^{\infty} c_{ru}(k\tilde{T}_{ru} + \tau_0) \alpha_k(\tau - \tau_0; \tilde{T}_{ru}) \quad (3.29)$$

in which $\tilde{T}_{ru} = 1/(2\tilde{f}_{ru})$ and $\tilde{f}_{ru} = \min(\tilde{f}_r, \tilde{f}_u)$. Indeed, the Fourier transform $s_{ru}(f)$ of $c_{ru}(\tau)$, $r \neq u$, is zero outside the range $(-\tilde{f}_{ru}, \tilde{f}_{ru})$ such that Eq. (3.29) holds according to the sampling theorem in Eq. (2.1). The bandwidth $(-\tilde{f}_{ru}, \tilde{f}_{ru})$ of $s_{ru}(f)$ can be obtained from the spectral representation of the components r and u of $X(t)$ by direct calculations.

A direct consequence of this result is that $\underline{X}_N(t)$ is a version of $\underline{X}(t)$ asymptotically as $N_r \rightarrow \infty$, $r = 1, \dots, p$, provided that $\underline{X}(t)$ is a Gaussian process. In this case, $\underline{X}_N(t)$ is also Gaussian and the finite dimensional distributions of $\underline{X}(t)$ and $\underline{X}_N(t)$ are defined by their second-moment characteristics uniquely and the first two moments of these processes coincide asymptotically as $N_r \rightarrow \infty$, $r = 1, \dots, p$.

A local representation as in Sec. 3.1.2. can be developed for $\underline{X}(t)$. Consider the processes

$$Y_{r,n_r} = \sum_{k=n_{r,t}-n_r}^{n_{r,t}+n_r+1} X_{r,k} \alpha_k(t; T_r) \quad (3.30)$$

$$r = 1, \dots, p$$

$$n_{r,t} T_r \leq t \leq (n_{r,t}+1)T_r$$

in which n_r is a specified positive integer defining the size of the window for the r -th component of $\underline{X}(t)$ and $n_{r,t} = [t/T_r]$ = the largest integer smaller than t/T_r . The representation depends on $2(n_r+1)$ values of $X_r(t)$ that are located symmetrically about the cell $[n_{r,t} T_r, (n_{r,t}+1) T_r]$ containing the current time t . The processes $Y_{r,n_r}(t)$ have the same asymptotic properties as $X_{r,N_r}(t)$ in Eq. (3.23) as $n_r \rightarrow \infty$, $r = 1, \dots, p$. Therefore,

$$\underline{Y}_n(t) = \begin{bmatrix} Y_{1,n_1}(t) \\ \vdots \\ Y_{p,n_p}(t) \end{bmatrix} \quad (3.31)$$

can be used to generate realizations of $\underline{X}(t)$, in which $\underline{n} = (n_1, \dots, n_p)'$. As in the case of random processes, the size of the windows n_r , $r = 1, \dots, p$, determines the number of random variables $\sum_{r=1}^p 2(n_r+1)$ involved in the

representation $\underline{Y}_{\underline{n}}(t)$ of $\underline{X}(t)$ and the accuracy of the representation. The model $\underline{Y}_{\underline{n}}(t)$ is a nonstationary process for any \underline{n} . However, it is nearly stationary when the components n_r , $r = 1, \dots, p$, of \underline{n} are larger than 5 or 10, as demonstrated in figures 4-4 and 4-5.

3.3. Random Fields ($q > 1$, $p = 1$)

Let $X(\underline{t})$ be a real-valued, zero-mean, homogeneous Gaussian random field defined on R^q with covariance function $c(\underline{\tau}) = E X(\underline{t} + \underline{\tau}) X(\underline{t})$ and mean power spectral density $s(\underline{f}) = \int_{R^q} e^{-i2\pi \underline{f}' \underline{\tau}} c(\underline{\tau}) d\underline{\tau}$, [1]. It is assumed that the power of $X(\underline{t})$ is concentrated in the interval $\prod_{s=1}^q (-\bar{f}_s, \bar{f}_s)$, $\bar{f}_s = \bar{f}_{1s}$, $0 < \bar{f}_s < \infty$, $s = 1, \dots, q$.

Consider the family of parametric random fields

$$X_{\underline{N}}(\underline{t}) = \sum_{k_1=-N_1}^{N_1} \dots \sum_{k_q=-N_q}^{N_q} X_{k_1, \dots, k_q} \prod_{s=1}^q \alpha_{k_s}(t_s; T_s) \quad (3.32)$$

in which $\underline{N} = (N_1, \dots, N_q)'$, $T_s = 1/(2\bar{f}_s)$, $s = 1, \dots, q$, and $X_{k_1, \dots, k_q} = X(k_1 T_1, \dots, k_q T_q)$. The random field depends on a finite number of variables for $N_s < \infty$, $s = 1, \dots, q$, that coincide with the values of the field at the nodal points $(k_1 T_1, \dots, k_q T_q)$, $k_s = -N_s, \dots, 0, \dots, N_s$; $s = 1, \dots, q$. The parametric fields $X_{\underline{N}}(\underline{t})$ and $X(\underline{t})$ take on the same values at the nodal points for any value of \underline{N} provided that $t_s \in [-N_s T_s, N_s T_s]$, $s = 1, \dots, q$.

Proposition 7. $X_{\underline{N}}(\underline{t})$ has the same first two moments as $X(\underline{t})$ asymptotically as $N_s \rightarrow \infty$, $s = 1, \dots, q$.

The mean of $X_{\underline{N}}(\underline{t})$ is zero for any $\underline{t} \in R^q$ and \underline{N} because $E X(\underline{t}) = 0$. The covariance function of two parametric fields $X_{\underline{N}}(\underline{t})$ and $X_{\underline{M}}(\underline{t})$ is

$$\begin{aligned}
 c_{\underline{N}, \underline{M}}(\underline{t+r}, \underline{t}) &= E X_{\underline{N}}(\underline{t+r}) X_{\underline{M}}(\underline{t}) \\
 &= \sum_{k_1=-N_1}^{N_1} \dots \sum_{k_q=-N_q}^{N_q} \prod_{s=1}^q \alpha_{k_s}(t_s+r_s; T_s) \\
 &\quad * \sum_{\ell_1=-M_1}^{M_1} \dots \sum_{\ell_q=-M_q}^{M_q} c((k_1-\ell_1)T_1, \dots, (k_q-\ell_q)T_q) \prod_{r=1}^q \alpha_{\ell_r}(t_r; T_r)
 \end{aligned} \tag{3.33}$$

From Eq. (2.4), the condition $c(\underline{r}) = c(-\underline{r})$ that is satisfied by the covariance function of $X(\underline{t})$, and the fact that the Fourier transform $s(\underline{f})$ of $c(\underline{r})$ is zero outside the interval $\prod_{s=1}^q (-\hat{f}_s, \hat{f}_s)$, one finds that

$$\begin{aligned}
 &\lim_{\substack{M_r \rightarrow \infty \\ r=1, \dots, q}} c_{\underline{N}, \underline{M}}(\underline{t+r}, \underline{t}) \\
 &= \sum_{k_1=-N_1}^{N_1} \dots \sum_{k_q=-N_q}^{N_q} c(t_1-k_1T_1, \dots, t_q-k_qT_q) \prod_{s=1}^q \alpha_{k_s}(t_s+r_s; T_s)
 \end{aligned} \tag{3.34}$$

Moreover, the expression in Eq. (3.34) approaches $c(\underline{r})$ as $N_s \rightarrow \infty$, $s = 1, \dots, q$, as demonstrated by the result in Eq. (2.4). This proves the statement in the proposition.

It can be noted from Eq. (3.33) that $X_{\underline{N}}(\underline{t})$ is an inhomogeneous random field for any finite values of N_s , $s = 1, \dots, q$. However, it is nearly homogeneous even for small values of these parameters, as it is demonstrated by examples in the next section.

Proposition 8. Random field $X_{\underline{N}}(\underline{t})$ approaches $X(\underline{t})$ in the mean square sense as $N_s \rightarrow \infty$, $s = 1, \dots, q$, for any $\underline{t} \in R^q$.

Direct calculations following the approach in the previous proposition show that

$$\lim_{\substack{N_s \rightarrow \infty \\ s=1, \dots, q}} E(X_{\underline{N}}(\underline{t}) - X(\underline{t}))^2 = 0 \quad (3.35)$$

which proves the statement in the proposition.

A consequence of the last two propositions is that $X_{\underline{N}}(\underline{t})$ is a version of $X(\underline{t})$ asymptotically as $N_s \rightarrow \infty$, $s = 1, \dots, q$, when $X(\underline{t})$ is Gaussian. Indeed, the first two moments of $X_{\underline{N}}(\underline{t})$ and $X(\underline{t})$ coincide as $N_s \rightarrow \infty$, $s=1, \dots, q$. Therefore, the finite dimensional distributions of these processes are identical because $X(\underline{t})$ is a Gaussian field.

Propositions 7 and 8 demonstrate that $X_{\underline{N}}(\underline{t})$ is a viable approximation of $X(\underline{t})$. The accuracy of the approximation increases with its order \underline{N} , i.e., as parameters N_s , $s = 1, 2, \dots, q$, take on larger values. The mean square error of an approximating field can be obtained from the expectation in Proposition 8 by following the approach in Eqs. (3.8) and (3.9). It was shown that $X_{\underline{N}}(\underline{t})$ becomes a version of $X(\underline{t})$ asymptotically as $N_s \rightarrow \infty$, $s = 1, \dots, q$, when the field is Gaussian. This property cannot be extended to non-Gaussian random fields. Although $X_{\underline{N}}(\underline{t})$ and $X(\underline{t})$ coincide at the nodal points, it is difficult to find the distribution of $X_{\underline{N}}(\underline{t})$ at arguments \underline{t} different from the nodes when $X(\underline{t})$ is a non-Gaussian random field.

Consider the family of parametric random fields

$$Y_{\underline{n}}(\underline{t}) = \sum_{k_1=n_1(\underline{t})-n_1}^{n_1(\underline{t})+n_1+1} \cdots \sum_{k_q=n_q(\underline{t})-n_q}^{n_q(\underline{t})+n_q+1} X_{k_1, \dots, k_q} \prod_{s=1}^q \alpha_{k_s}(t_s; T_s)$$

$$\underline{t} \in \prod_{s=1}^q [n_s(\underline{t}) T_s, (n_s(\underline{t}) + 1) T_s] \quad (3.36)$$

defining local representations of $X(\underline{t})$, in which $n_s(\underline{t}) = [t_s/T_s]$ = the largest integer smaller than t_s/T_s and n_s , $s = 1, \dots, q$, are chosen positive integers defining the size of a window centered on the cell $\prod_{s=1}^q [n_s(\underline{t})T_s, (n_s(\underline{t})+1)T_s]$ which contains the current value of argument \underline{t} . The window includes all nodal values of $X(\underline{t})$ in Eq. (3.36).

The local representation in Eq. (3.36) has similar properties as $X_{\underline{N}}(\underline{t})$ in Eq. (3.32). It coincides with the field $X(\underline{t})$ at every nodal point in the window. The field $Y_{\underline{n}}(\underline{t})$ has the same mean and covariance function as $X(\underline{t})$ asymptotically as $n_s \rightarrow \infty$, $s = 1, \dots, q$. Moreover, $Y_{\underline{n}}(\underline{t})$ is a version of $X(\underline{t})$ as $n_s \rightarrow \infty$, $s = 1, \dots, q$, when $X(\underline{t})$ is Gaussian.

However, there is a significant difference between the approximations of $X(\underline{t})$ in Eqs. (3.32) and (3.36). Although they both involve values of $X(\underline{t})$ equally spaced at $T_s = 1/(2f_s)$, $s = 1, \dots, q$, these values are centered about the origin for $X_{\underline{N}}(\underline{t})$ and about \underline{t} for $Y_{\underline{n}}(\underline{t})$. As the norm of \underline{t} increases the order \underline{N} of $X_{\underline{N}}(\underline{t})$ must also increase such that the rectangle $\prod_{s=1}^q (-N_s T_s, N_s T_s)$ includes \underline{t} and $X_{\underline{N}}(\underline{t})$ accurately approximates $X(\underline{t})$. On the other hand, the representation $Y_{\underline{n}}(\underline{t})$ involves $\prod_{s=1}^q [2(n_s+1)]$ values of $X(\underline{t})$ for all \underline{t} . This feature is particularly useful in simulation studies.

3.4. Vector Random Fields ($q > 1, p > 1$)

Suppose that $\underline{X}(\underline{t})$ is a vector random field defined in \mathbb{R}^q with values on \mathbb{R}^p .

The field is homogeneous with mean zero covariance functions $c_{ru}(\underline{t}) = E X_r(\underline{t} + \underline{t}) X_u(\underline{t})$ and power spectral densities $s_{ru}(\underline{f}) = \int_{\mathbb{R}^q} e^{-i2\pi \underline{f}' \underline{t}} c_{ru}(\underline{t}) d\underline{t}$, $r, u = 1, \dots, p$. It is assumed that the power of component $X_r(\underline{t})$ of the field is concentrated in $\prod_{s=1}^q (-\hat{f}_{rs}, \hat{f}_{rs})$, $0 < \hat{f}_{rs} < \infty$, $r = 1, \dots, q$.

The extension of the results in the previous sections to vector random fields can be based on considerations similar to those in Sec. 3.2. Indeed, the components $X_r(\underline{t})$ of $\underline{X}(\underline{t})$, $r = 1, \dots, p$, are real-valued band-limited random fields such that results in Sec. 3.3 apply to each of these components.

Therefore, the models

$$X_{r, \underline{N}(r)}(\underline{t}) = \sum_{k_1 = -N_{r1}}^{N_{r1}} \dots \sum_{k_q = -N_{rq}}^{N_{rq}} X_r(k_1 T_{r1}, \dots, k_q T_{rq}) \prod_{s=1}^q \alpha_{k_s}(t_s; T_{rs}), \quad (3.37)$$

in which $\underline{N}(r) = (N_{r1}, \dots, N_{rq})'$ and $T_{rs} = 1/(2\hat{f}_{rs})$ and

$$Y_{r, \underline{n}(r)}(\underline{t}) = \sum_{k_1 = -n_{r1}(\underline{t}) - n_{r1}}^{n_{r1}(\underline{t}) + n_{r1} + 1} \dots \sum_{k_q = -n_{rq}(\underline{t}) - n_{rq}}^{n_{rq}(\underline{t}) + n_{rq} + 1} X_r(k_1 T_{r1}, \dots, k_q T_{rq}) \prod_{s=1}^q \alpha_{k_s}(t_s; T_{rs})$$

$$\underline{t} \in \prod_{s=1}^q [n_{rs}(\underline{t}) T_{rs}, (n_{rs}(\underline{t}) + 1) T_{rs}], \quad (3.38)$$

in which $n_{rs}(\underline{t}) = [t/T_{rs}]$ - the largest integer smaller than t/T_{rs} and n_{rs} - positive integers, approach $X_r(\underline{t})$, $r = 1, \dots, q$, in the mean square sense as $N_{rs} \rightarrow \infty$ and $n_{rs} \rightarrow \infty$, $s = 1, \dots, q$, respectively. It is also possible to show that the vector random fields with components $X_{r, \underline{N}(r)}(\underline{t})$ and $Y_{r, \underline{n}(r)}(\underline{t})$

converge in the mean square sense to $\underline{X}(\underline{t})$ as N_{rs} and n_{rs} approach infinity, respectively, $r = 1, \dots, p$; $s = 1, \dots, q$.

SECTION 4
SIMULATION ALGORITHMS

The local representations in Eqs. (3.19), (3.30), (3.36) and (3.38) are used to generate realizations of a zero-mean stationary Gaussian random function $\underline{X}(\underline{t}) \in R^p$, $\underline{t} \in R^q$, for $q = 1$, $p = 1$; $q = 1$, $p > 1$; $q > 1$, $p = 1$; and $q > 1$, $p > 1$. The local representations involve a fixed number of random variables that are equal to the values of the random function at a set of nodal points. The set of nodal points is determined by the size of the window considered in the representation and the value of argument \underline{t} .

4.1. Random Processes ($q = 1$, $p = 1$)

Consider an instant t , the corresponding cell $[n_t T, (n_t + 1)T]$, and the local approximation $Y_n(t)$ of order n in Eq. (3.19). Suppose that a sample

$$y_n(t) = \sum_{k=n_t-n}^{n_t+n+1} x_k \alpha_k(t; T) \quad (4.1)$$

of $Y_n(t)$ is available in the cell. It involves realizations x_k of the nodal values X_k of the process $X(t)$ included in the window $[(n_t - n)T, (n_t + n + 1)T]$.

The objective is to extend the sample $y_n(t)$ of $Y_n(t)$ in the next cell $[(n_t + 1)T, (n_t + 2)T]$. This extension depends on the nodal values X_k , $k = n_t - n + 1, \dots, n_t + n + 2$, of which the values $X_k = x_k$, $k \leq n_t + n + 1$, have already been generated. The only new nodal (random) value in the local representation of $X(t)$ over the cell $[(n_t + 1)T, (n_t + 2)T]$ is $X_{n_t + n + 2}$. Therefore, the generated sample of $X_{n_t + n + 2}$ should be conditioned on $X_k = x_k$, $k \leq n_t + n + 1$. In the proposed algorithm for simulation the condition is limited to the width of the window such that the new nodal value is a sample of the random variable

$X_{n_t+n+2}^* = X_{n_t+n+2} \mid \{X_k = x_k, \quad k = n_t-n, \dots, n_t+n+1\}$. Efficient methods are available for generating samples of conditional Gaussian variables (Appendix). The generation of the nodal values for the subsequent cells can be performed sequentially when time t crosses from one cell to another. The storage requirement is minimal because only $2(n+1)$ values need to be recorded at any time t . This constitutes a major advantage over the simulation method based on a discrete spectral representation of $X(t)$ that requires storage of realizations of many random variables. Moreover, the generation of samples of $X(t)$ is performed on line, similar to the simulation method based on the ARMA model. However, the definition of the local representation of $X(t)$ requires much less computation than for an ARMA model.

Example 1. Suppose that $X(t)$ is a band-limited white noise process with spectrum $s(f) = s_0$, $s_0 = 1.0$, for $f \in (-\tilde{f}, \tilde{f})$, $\tilde{f} = 0.5$, and zero otherwise. Covariances of the approximation $Y_n(t)$ of $X(t)$ are shown in figure 4-1 for $t/T = k, k+1/4, k+1/2$, and $k+3/4$, in which k is an integer.

Results in table 4-I and figure 4-2(a) are based on 5000 realization of $Y_n(t)$ for $n = 1$ and 3. They show, consistent with theoretical results in figure 4-1, that the variance of $Y_n(t)$ depends on the order n of the model.

Unsatisfactory estimates can be obtained for $n = 1$ when time t coincides with the mid point between consecutive nodes. On the other hand, the histograms follow closely the probability of $X(t)$ for all values of n .

The proposed simulation algorithm is particularly efficient when applied to estimate the probability $q(x)$ that a process $X(t)$ exceeds a high threshold x at an arbitrary instant. For example, suppose that $X(t)$ is a stationary band-

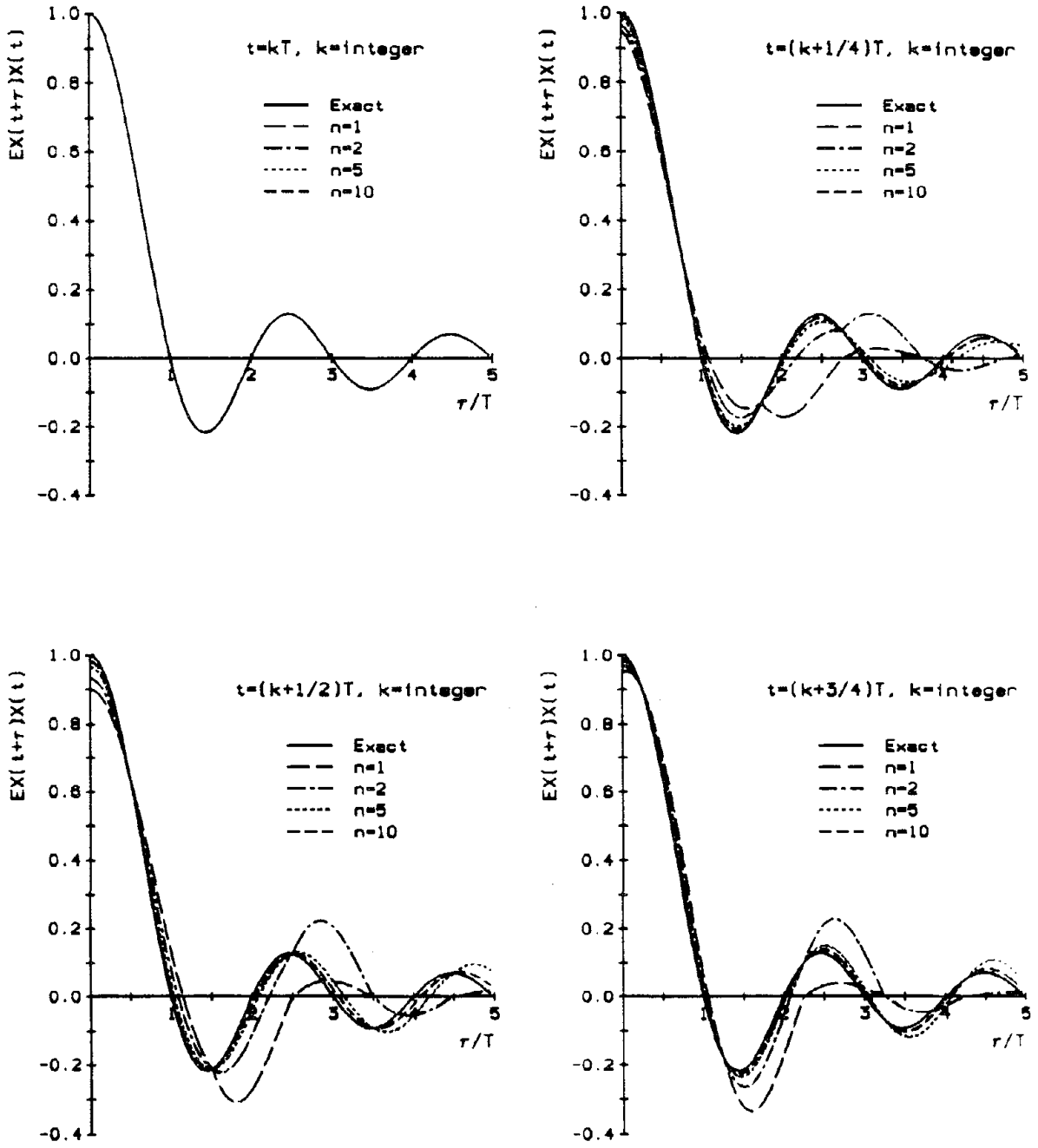
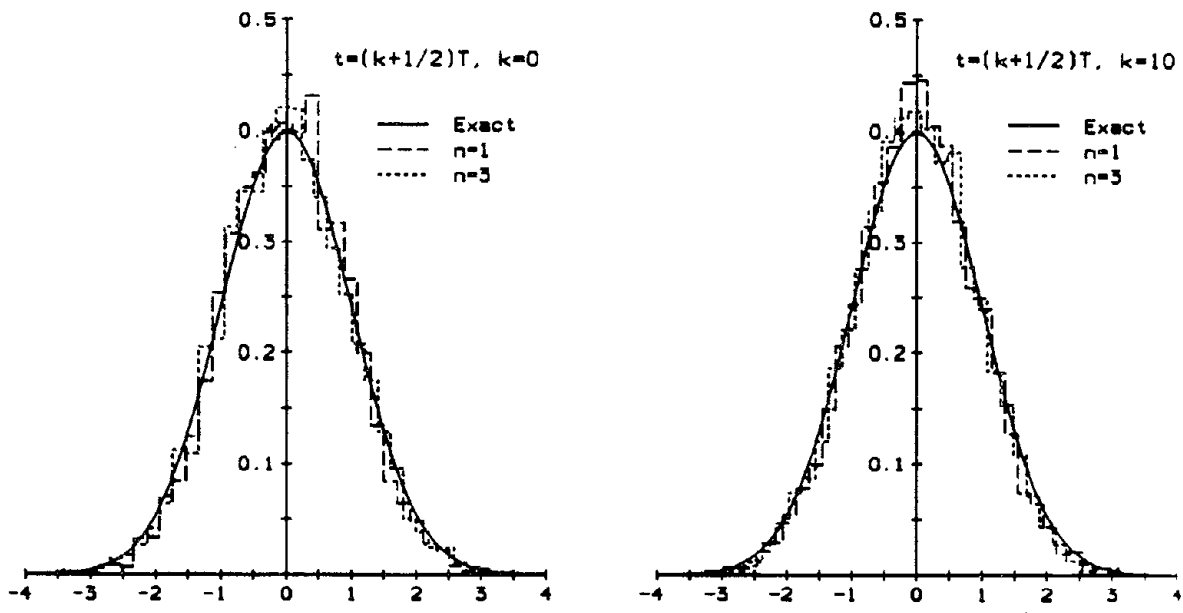
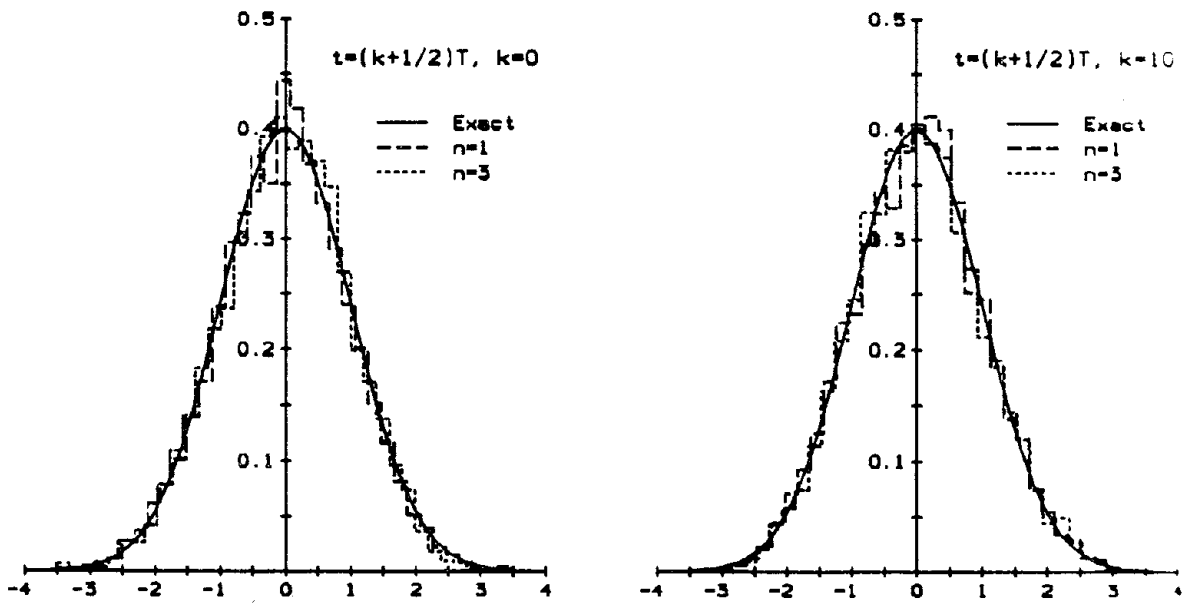


FIGURE 4-1 Covariance Functions of $Y_n(t)$ in Eq. (3.19) and $X(t)$ for a Band-Limited White Noise Process



(a) Band-Limited White Noise



(b) Truncated First Order Markov

FIGURE 4-2 Histograms of $Y_n(t)$ in Eq. (3.19) for Band-Limited White Noise and Truncated First Order Gauss-Markov Processes

TABLE 4-I Estimated Variances of $Y_n(t)$ for a Band-Limited White Noise

Time	Model $Y_n(t)$	
	n=1	n=3
0.0	0.9996	0.9888
0.25	0.9466	0.9433
0.50	0.8754	0.9087
0.75	0.9282	0.9455
10.0	0.9938	0.9670
10.25	0.9298	0.9433
10.50	0.8563	0.9337
10.75	0.9180	0.9713

limited Gaussian white noise with bandwidth $(0, 0.5)$, mean zero, and variance one. Estimates of $q(x)$ based on $Y_n(t)$ in Eq. 3.19 have errors of approximately 3% when $x = 5$, $n = 75$, and the sample size is infinity. On the other hand, a thousand harmonics with random phase are needed to achieve a 3% error in the estimates of $q(x)$ for $x = 5$ when the simulation is based on the spectral representation method and infinite sample size [15]. The computation times for generating a thousand 10 sec. long realizations of $X(t)$ are 63 and 15.80 minutes for the spectral representation method and the algorithm developed in this study, respectively.

Example 2. Similar results as in table 4-I and figure 4-2(a) are presented in table 4-II and figure 4-2(b) for a process $X(t)$ with power spectral density obtained by truncating the spectrum of a first order Gauss-Markov process. The spectrum $s(f)$ of $X(t)$ is proportional with $(4\pi^2 f^2 + \alpha^2)^{-1}$ for $f \in (-\bar{f}, \bar{f})$, $\bar{f} = 0.5$, and zero otherwise. It is scaled such that the variance of $X(t)$ be equal to one. Even the lower order model ($n=1$) provides a satisfactory

TABLE 4-II Estimated Variances for a Truncated First Order Gauss-Markov Process

Time	Model $Y_n(t)$	
	n=1	n=3
0.0	1.0163	0.9899
0.25	0.9994	0.9951
0.50	0.9975	0.9952
0.75	1.0336	1.0090
10.0	0.9652	0.9861
10.25	0.9699	0.9762
10.50	0.9862	0.9748
10.75	1.0301	0.9944

approximation for this process. Results correspond to 5000 realizations of $Y_n(t)$ and $\alpha = 2$. The improved representation relative to the case studied in Example 1 relates to differences in the frequency content of the band-limited white noise and the truncated Markov processes.

Example 3. The mean upcrossing rate of level x of $X(t)$ can be obtained from the Rice formula [3]

$$\nu(x) = \frac{\sqrt{\lambda_2}}{2\pi} \exp\left(-\frac{1}{2} x^2\right) \quad (4.2)$$

in which $\lambda_2 = (2\pi)^3 \int_{-\bar{f}}^{\bar{f}} f^2 s(f) df$. Simulation can also be used to obtain estimates $\nu_n(x)$ of $\nu(x)$ from realizations of the model $Y_n(t)$ in Eq. (3.11) of $X(t)$.

Figure 4-3(a) and table 4-III give the mean x -upcrossing rates $\nu(x)$ and $\nu_n(x)$ when $X(t)$ is the band-limited white noise process in Example 1. Figure 4-3(b)

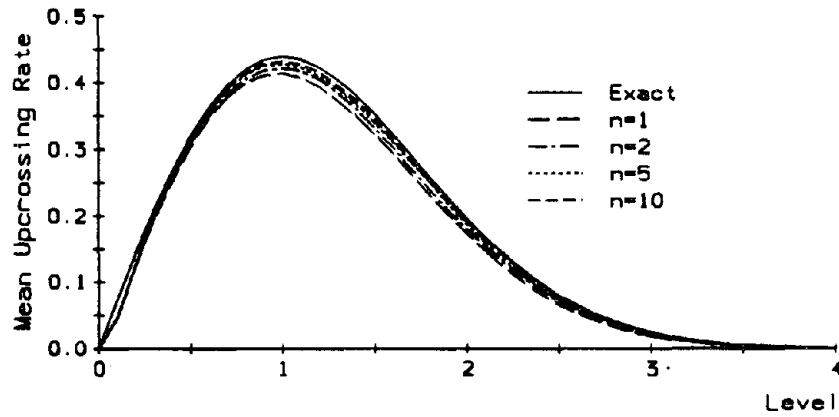
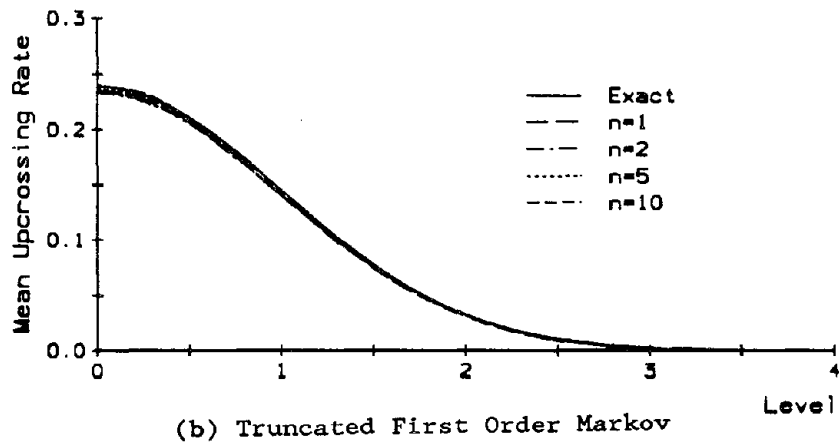
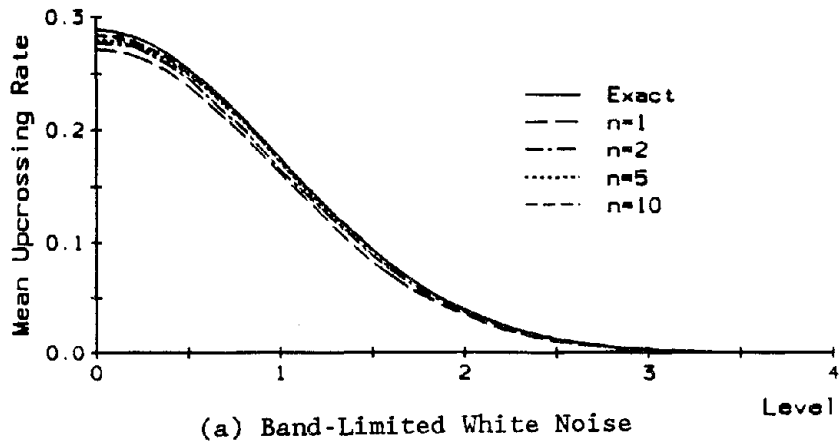


FIGURE 4-3 Mean Upcrossing Rates for Band-Limited White Noise, Truncated First Order Gauss-Markov, and Envelope of a Narrow Band Gaussian Process with Constant Power within a Small Frequency Range

TABLE 4-III Mean Upcrossing Rates for a Band-Limited Gaussian White Noise Process

Level x	Exact, $\nu(x)$ (Eq. 4.2)	Simulation based on $Y_n(t)$, $\nu_n(x)$			
		$n=1$	$n=2$	$n=5$	$n=10$
0.0	2.87×10^{-1}	2.71×10^{-1}	2.77×10^{-1}	2.80×10^{-1}	2.84×10^{-1}
1.0	1.75×10^{-1}	1.62×10^{-1}	1.65×10^{-1}	1.71×10^{-1}	1.73×10^{-1}
2.0	3.91×10^{-2}	3.44×10^{-2}	3.63×10^{-2}	3.79×10^{-2}	3.85×10^{-2}
3.0	3.21×10^{-3}	2.62×10^{-3}	3.10×10^{-3}	3.26×10^{-3}	3.34×10^{-3}

TABLE 4-IV Mean Upcrossing Rates for a Truncated First Order Gauss-Markov Process

Level x	Exact, $\nu(x)$ (Eq. 4.2)	Simulation based on $Y_n(t)$, $\nu_n(x)$			
		$n=1$	$n=2$	$n=5$	$n=10$
0.0	2.39×10^{-1}	2.35×10^{-1}	2.33×10^{-1}	2.37×10^{-1}	2.40×10^{-1}
1.0	1.45×10^{-1}	1.40×10^{-1}	1.40×10^{-1}	1.38×10^{-1}	1.43×10^{-1}
2.0	3.24×10^{-1}	3.05×10^{-2}	3.10×10^{-2}	3.18×10^{-2}	3.19×10^{-2}
3.0	2.66×10^{-3}	2.44×10^{-3}	2.30×10^{-3}	2.24×10^{-3}	2.14×10^{-3}

and table 4-IV show simulation results for the truncated Markov process in Example 2. The simulation results are based on 5000 realizations of $Y_n(t)$. The estimated mean upcrossing rates are satisfactory even for $n = 1$.

Example 4. Suppose that $X(t)$ is a zero mean stationary Gaussian process with a narrow band spectrum $s(f) = s_0 = 0.5$, for $|f \pm f_0| < \bar{f}$, $0 < \bar{f} \ll f_0$, $\bar{f} = 0.5$, $f_0 = 20$, and zero otherwise. The peaks of narrow band processes tend to cluster in time such that maxima of $X(t)$ can be estimated more accurately from upcrossings of the envelope $V(t)$ of the process defined in Eq. (3.12). It

can be shown that the mean v-upcrossing rate of V(t) is [3,4]

$$\nu^*(v) = \sqrt{\frac{\lambda_0 \lambda_2 - \lambda_1^2}{2\pi \lambda_0^2}} \frac{v}{\sqrt{\lambda_0}} \exp\left[-\frac{v^2}{2\lambda_0}\right] \quad (4.3)$$

in which $\lambda_k = \int_{-\infty}^{\infty} |2\pi f|^k s(f) df$, $k = 0, 1, \dots$, are spectral moments.

Let $\nu_n^*(v)$ be an estimate of $\nu^*(v)$ obtained from realizations of the n'th order local approximation of V(t) defined by

$$V_n(t) = \left[Y_{c,n}(t)^2 + Y_{s,n}(t)^2 \right]^{1/2} \quad (4.4)$$

in which $Y_{c,n}$ and $Y_{s,n}(t)$ are given in Eq. (3.21). Figure 4-3(c) and table 4-V show the mean rates $\nu^*(v)$ and $\nu_n^*(v)$ for several values of n. Satisfactory approximations are obtained for $\nu^*(v)$ when $n \geq 2$.

TABLE 4-V Mean Upcrossing Rates of the Envelope of a Narrow Band Gaussian Process

Level v	Exact, $\nu^*(v)$ (Eq. 4.3)	Simulation based on $V_n(t)$, $\nu_n^*(v)$			
		n=1	n=2	n=5	n=10
1.0	4.39×10^{-1}	4.13×10^{-1}	4.21×10^{-1}	4.28×10^{-1}	4.31×10^{-1}
2.0	1.96×10^{-1}	1.72×10^{-1}	1.79×10^{-1}	1.86×10^{-1}	1.92×10^{-1}
3.0	2.71×10^{-2}	1.80×10^{-2}	1.93×10^{-2}	2.21×10^{-2}	2.27×10^{-2}
4.0	9.71×10^{-4}	4.60×10^{-4}	6.80×10^{-3}	8.20×10^{-4}	6.60×10^{-4}

4.2. Vector Random Processes ($q = 1, p > 1$)

Consider an instant t , the corresponding cells $[n_{r,t} T_r, (n_{r,t}+1)T_r]$, $r = 1, \dots, p$, and the local representations $Y_{r,n}(t)$, $r = 1, \dots, p$, in Eq. (3.30) depending on the nodal values $X_{r,k}$, $k = n_{r,t}-n_r, \dots, n_{r,t}+n_r+1$, $r = 1, \dots, p$. The generation of samples of $\underline{X}(t)$ based on these representations can pose minor bookkeeping problems when the nodal intervals T_r do not coincide for all components. Two cases are examined.

Case 1 ($T_r = T; r = 1, \dots, p$). The parameters $n_{r,t} = n_t$ have the same values for all components because $T_r = T$, $r = 1, \dots, p$. The window sizes n_r may depend on the component. However, the same window size $n_r = n$, $r = 1, \dots, p$, is used for all components.

Let t be an instant in cell $[n_t T, (n_t+1)T]$ and $y_{\underline{n}}(t)$ a realization of $Y_{\underline{n}}(t)$ in this cell depending on the nodal values $\underline{X}((n_t+n+1)T) = \underline{x}_1; \dots; \underline{X}((n_t-n)T) = \underline{x}_{2(n+1)}$ of $\underline{X}(t)$. The extension of $y_{\underline{n}}(t)$ in the next cell $[(n_t+1)T, (n_t+2)T]$ involves a sample of random vector $\underline{X}((n_t+n+2)T)$. This sample depends on the previously generated nodal values of the process. For simplicity, the condition is only extended over the width of the window, i.e., a sample of $\underline{X}^*((n_t+n+2)T) = \underline{X}((n_t+n+2)T) \mid \{\underline{X}((n_t+n+1)T) = \underline{x}_1, \dots, \underline{X}((n_t-n+1)T) = \underline{x}_{2n+1}\}$ is used in simulation. The generation of such conditional samples can be performed efficiently by the algorithm in the Appendix.

Case 2 (General): The nodal points and window sizes differ from component to component. Consider first the special case in which the periods T_r do not differ significantly. Let

$$T = \min_{1 \leq r \leq p} (T_r) \quad (4.5)$$

and take $n_r = n$, $r = 1, \dots, p$. Simulation of samples of $\underline{X}(t)$ can be based on the representation in Eq. (3.30) with T_r replaced by T in Eq. (4.5) and the approach in Case 1. The replacement of T_r by T in Eq. (4.5) is valid because it corresponds to a sampling rate that is equal or higher than the minimum required rate. This approach can be applied in all situations. However, it may become inefficient when the components of $\underline{X}(t)$ have significantly different bandwidths.

Consider now the more general case in which the nodal intervals T_r satisfy the conditions

$$T_1 \geq T_2 \geq \dots \geq T_p \quad (4.6)$$

and

$$T_r = \frac{T_{r-1}}{m_{r,r-1}}, \quad r = 1, \dots, p \quad (4.7)$$

where $m_{r,r-1}$ are positive integers and $m_{1,0} = 1$. The condition in Eq. (4.6) can always be satisfied by renumbering the components of $\underline{X}(t)$. On the other hand, Eq. (4.7) is not generally true. However, it can be validated if the bandwidths of the components of $\underline{X}(t)$ are adequately increased. From Eqs. (4.6) and (4.7), there are instances at which all components have nodes and the period of these instances is T_1 . The simulation algorithm can consist of cycles of duration T_1 . Let t_0 be an instant at which all nodes coincide. The algorithm starts by generating realizations of components $X_r(t)$ in the cells (t_0, t_0+T_r) , $r = 1, \dots, p$. Then, the realization of $X_p(t)$ is extended in the next $m_{p,p-1}$ cells of length T_p until the next node of component $X_{p-1}(t)$.

The next step is to extend the realization of $X_{p-1}(t)$ one step ahead in cell $(t_0+T_{p-1}, t_0+2T_{p-1})$. The process continues until realizations are obtained for components $\{X_2(t), \dots, X_p(t)\}$ in $[t_0, t_0+T_1]$. This constitutes the end of a simulation cycle.

Example 1. Consider the zero-mean bivariate Gaussian process $\underline{X}(t)$ with components

$$X_r(t) = \sqrt{1-\rho} Y_r(t) + \sqrt{\rho} Y(t), \quad 0 < \rho < 1, \quad r = 1, 2 \quad (4.8)$$

in which $Y_r(t)$, $r = 1, 2$, and $Y(t)$ are independent zero-mean, unit-variance stationary Gaussian processes. The power spectral densities $s_{Y_r}(f)$, $r = 1, 2$, and $s_Y(f)$ of these processes are constant and equal to $s_r = 1/(4\pi f_r^*)$, $r = 1, 2$, and $s = 1/(4\pi f^*)$ in $(-f_r^*, f_r^*)$ and $(-f^*, f^*)$, respectively, and zero outside these frequency bands. The corresponding covariance functions are

$$c_{Y_r}(\tau) = E Y_r(t+\tau) Y_r(t) = \frac{\sin(2\pi f_r^* \tau)}{2\pi f_r^* \tau}, \quad r = 1, 2$$

$$c_Y(\tau) = E Y(t+\tau) Y(t) = \frac{\sin(2\pi f^* \tau)}{2\pi f^* \tau} \quad (4.9)$$

The covariance functions $c_{ru}(\tau) = E X_r(t+\tau) X_u(t)$, $r, u = 1, 2$, of the components of $\underline{X}(t)$ are

$$c_{rr}(\tau) = (1-\rho) c_{Y_r}(\tau) + c_Y(\tau), \quad r = 1, 2$$

$$c_{ru}(\tau) = \rho c_Y(\tau), \quad r, u = 1, 2, \quad r \neq u \quad (4.10)$$

so that the corresponding power spectral densities can be obtained from

$$\begin{aligned}
s_{rr}(f) &= (1-\rho) s_{Y_r}(f) + \rho s_Y(f) \quad , \quad r = 1, 2 \\
s_{ru}(f) &= \rho s_Y(f) \quad , \quad r, u = 1, 2, \quad r \neq u
\end{aligned} \tag{4.11}$$

Therefore, the components $X_r(t)$ of $\underline{X}(t)$ have power in the frequency band $(-\bar{f}_r, \bar{f}_r)$, where $\bar{f}_r = \max \{f_r^*, f^*\}$, $r = 1, 2$.

Figure 4-4 shows exact and approximate covariance functions $c_{ru}(\tau)$ for $f_1^* = 1.0$, $f_2^* = 0.2$, and $f^* = 0.1$ for a medium correlation of the components $X_1(t)$ and $X_2(t)$, $\rho = 0.5$. The approximate covariance functions correspond to the local representation in Eq. (3.30) with $T_1 = 1/(2\bar{f}_1) = 0.5$, $T_2 = 1/(2\bar{f}_2) = 2.5$, window sizes $n = 1, 2, 5, 10$, and instances t coinciding with the nodes and the mid points between consecutive nodes. Consistent with Proposition 5 the approximate covariance functions approach the exact values $c_{ru}(\tau)$ as the window size n increases. The convergence is faster at instances t coinciding with nodal points.

Example 2. Consider the same vector random process as in Example 1 and a safe set $D = \{(x_1, x_2) : x_i \leq a_i, i = 1, 2\}$, where a_i are specified thresholds. It can be shown that the mean rate at which $\underline{X}(t)$ crosses out of D , or the mean D -outcrossing rate of $\underline{X}(t)$ is [17]

$$\nu(D) = \nu_1(a_1) [1 - \Phi(\alpha a_1 + \beta a_2)] + \nu_2(a_2) \Phi(d) \tag{4.12}$$

in which

$$\begin{aligned}
\alpha &= \rho / \sqrt{1-\rho^2} \quad , \quad \beta = -1/\sqrt{1-\rho^2} \\
d^2 &= \left[a_1 - \alpha a_2 / \sqrt{1+\alpha^2} \right]^2 + \left[\alpha a_1 + \beta a_2 + a_2 / \sqrt{1+\alpha^2} \right]^2
\end{aligned}$$

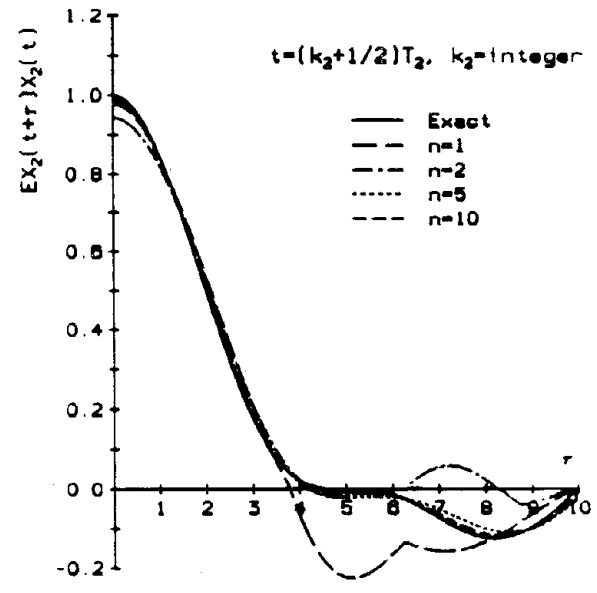
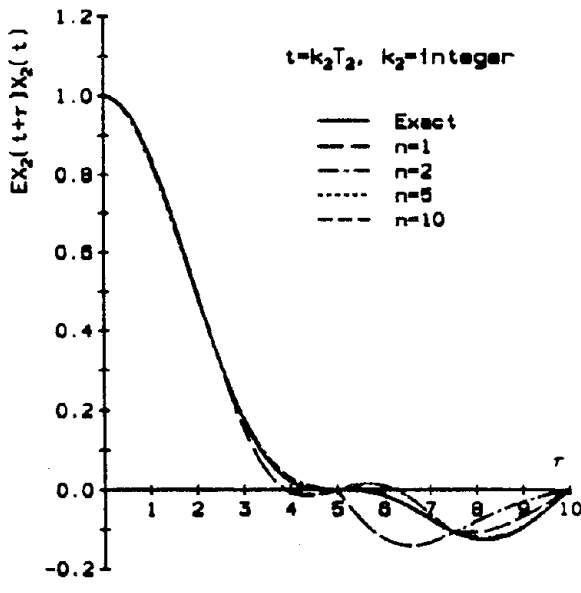
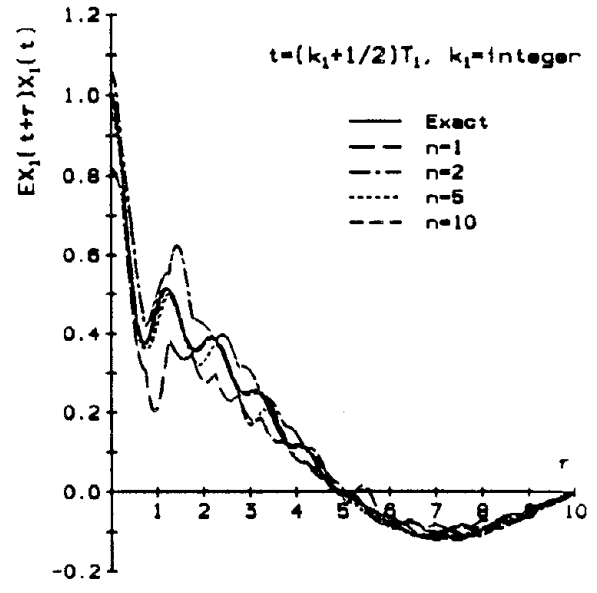
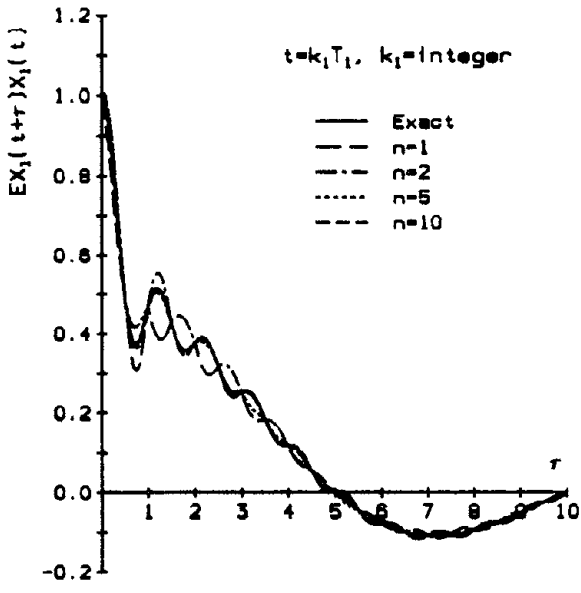


FIGURE 4-4 Covariance Functions of $\underline{Y}_n(t)$ in Eq. (3.30) and $\underline{X}(t)$ for the Bivariate Gaussian Process $\underline{X}(t)$ in Eq. (4.8) with $\rho = 0.5$

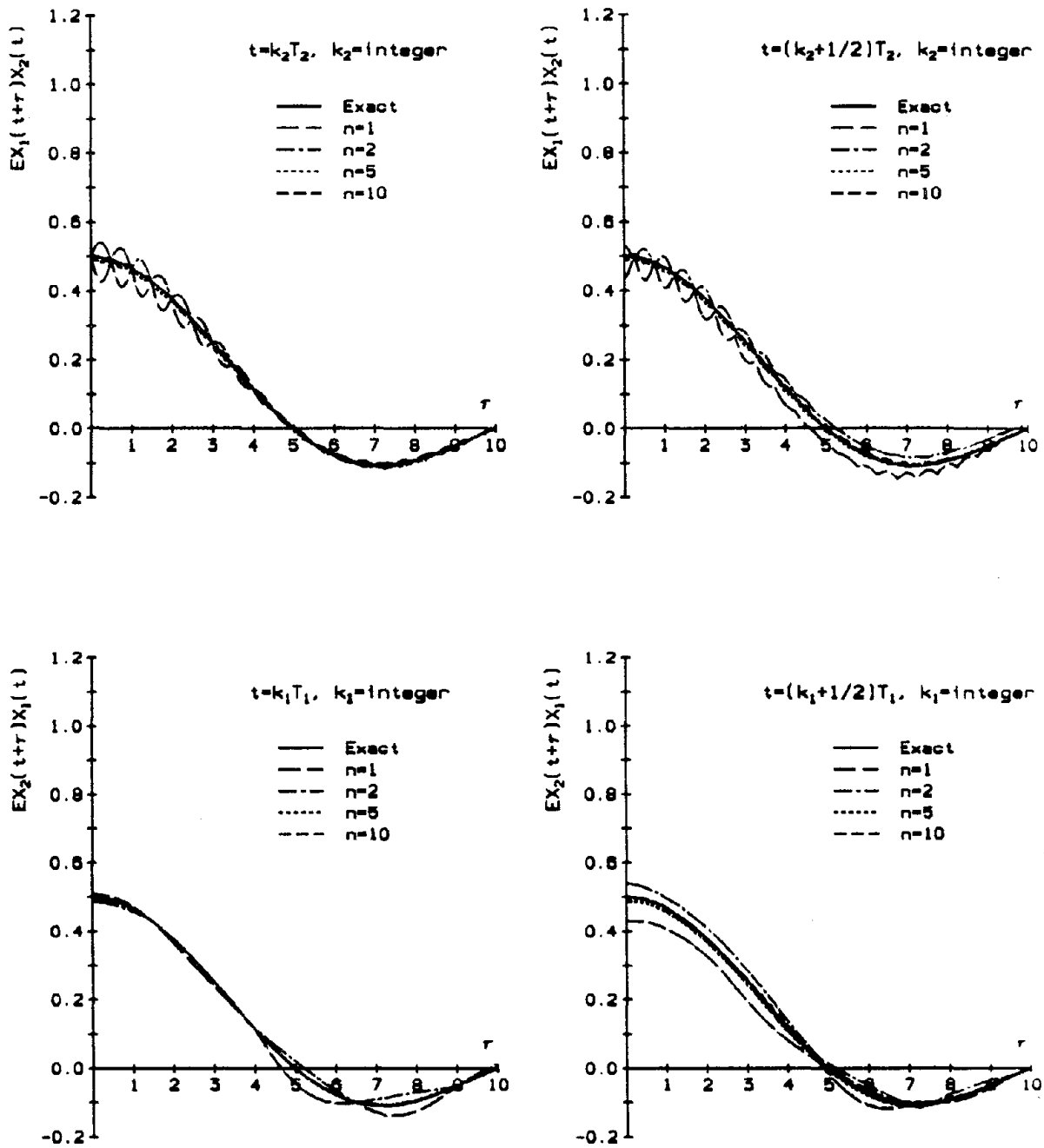


FIGURE 4-4 Covariance Functions of $\underline{Y}_n(t)$ in Eq. (3.30) and $\underline{X}(t)$ for the Bivariate Gaussian Process $\underline{X}(t)$ in Eq. (4.8) with $\rho = 0.5$

$$\nu_1(a_1) = \frac{1}{2\pi} \sqrt{E \dot{X}_1(t)^2} \exp \left[-\frac{1}{2} a_1^2 \right]$$

$$\nu_2(a_2) = \frac{1}{2\pi} \sqrt{\frac{E \dot{Z}(t)^2}{E Z(t)^2}} \exp \left[-\frac{1}{2} \frac{a_2^2}{E Z(t)^2} \right]$$

$$Z(t) = (\alpha Z_1(t) - Z_2(t)) / \sqrt{1 + \alpha^2}$$

$$Z_1(t) = X_1(t) \quad , \quad Z_2(t) = \alpha X_1(t) + \beta X_2(t) \quad (4.13)$$

Table 4-VI gives values of $\nu(D)$ in Eq. (4.12) and estimates of this mean D-outcrossing rate obtained from 10,000 samples of $X(t)$ generated from the local model $\underline{Y}_n(t)$ in Eq. (4.8). Results are for $(a_1, a_2) = (3, 3); (2, 3); (3, 2);$ and $(2, 2)$ and $\rho = 0.9999; 0.5$. The estimates of $\nu(D)$ can be obtained by calculating the rate of D-outcrossings for each sample of $\underline{X}(t)$ and averaging this rate over the ensemble of samples. A sample of $\underline{X}(t)$ has a D-outcrossing in a small time interval $(t, t+\Delta t)$ when $\underline{X}(t) \in D$ and $\underline{X}(t+\Delta t) \notin D$.

TABLE 4-VI Mean D-Outcrossing Rates of $\underline{X}(t)$

(a_1, a_2)	$\rho = 0.9999$				$\rho = 0.5$			
	Simulation			Exact	Simulation			Exact
	n=2	n=5	n=10		n=2	n=5	n=10	
(3,3)	.00378	.00148	.00068	.00065	.00610	.00493	.00532	.00534
(2,3)	.02975	.01321	.00948	.00849	.05736	.05289	.05625	.05567
(3,2)	.01051	.00799	.00782	.00782	.01583	.01498	.01498	.01550
(2,2)	.03377	.01446	.00812	.00792	.06236	.05810	.06024	.05946

Example 3. Consider another bivariate Gaussian process $\underline{X}(t)$ whose components satisfy the stochastic differential equations

$$\frac{d}{dt} \begin{bmatrix} X_1(t) \\ X_2(t) \end{bmatrix} = \begin{bmatrix} -\rho_1 & 0 \\ 0 & -\rho_2 \end{bmatrix} \begin{bmatrix} X_1(t) \\ X_2(t) \end{bmatrix} + \begin{bmatrix} 1 \\ 1 \end{bmatrix} W(t) \quad (4.14)$$

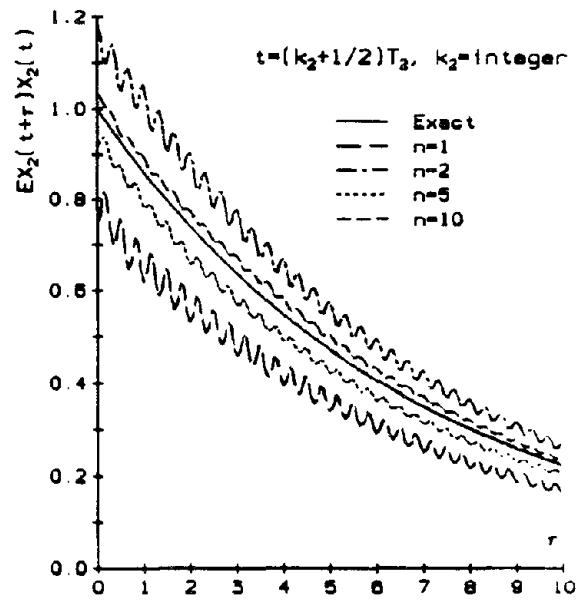
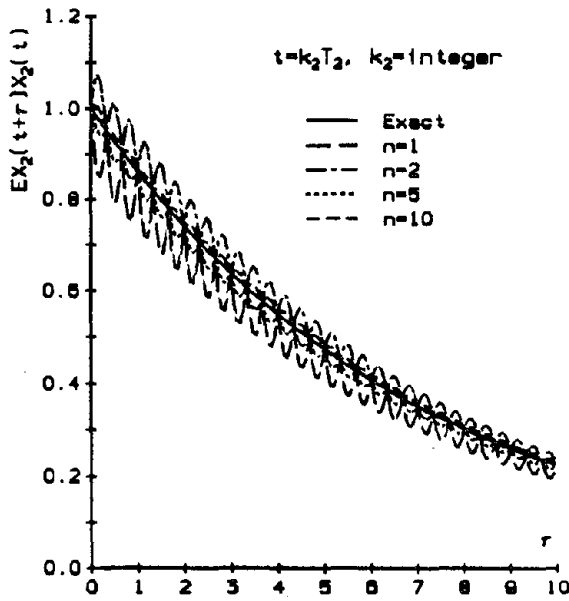
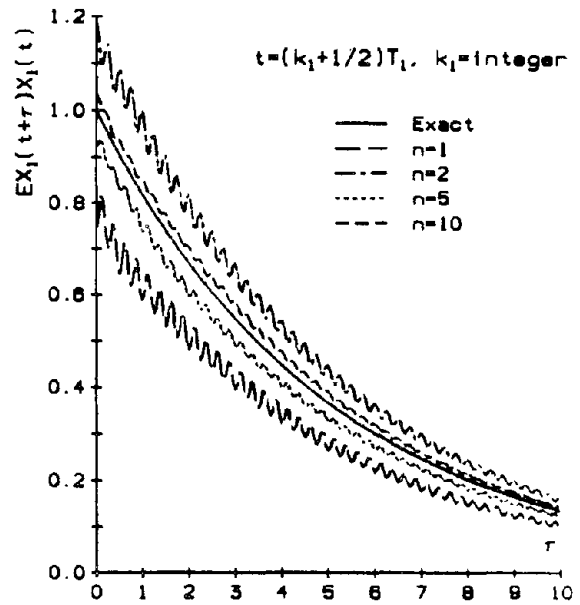
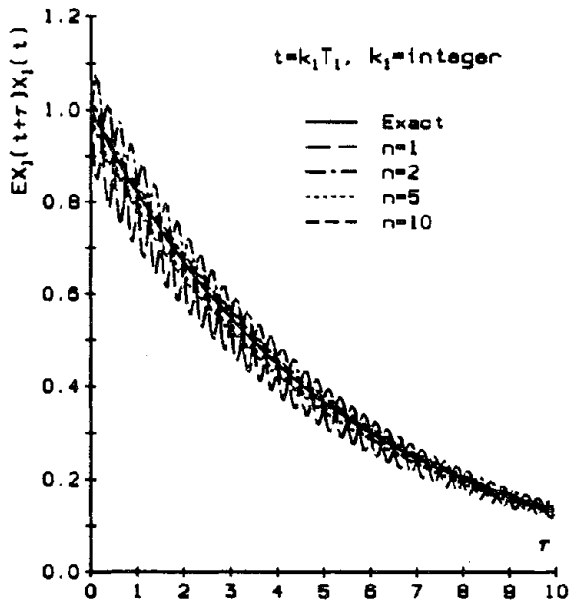
in which $\rho_r > 0$, $r = 1, 2$, and $W(t)$ is a zero-mean stationary Gaussian white noise process with covariance function $c_w(\tau) = c_0 \delta(\tau)$. Direct calculations show that the covariance and power spectral density functions of the stationary components of $\underline{X}(t)$ are

$$\begin{aligned} c_{rr}(\tau) &= \frac{c_0}{2\rho_r} e^{-\rho_r |\tau|}, \quad r = 1, 2 \\ c_{12} &= \frac{c_0}{\rho_1 + \rho_2} \begin{cases} e^{-\rho_1 \tau} & , \quad \tau > 0 \\ e^{\rho_2 \tau} & , \quad \tau < 0 \end{cases} \\ c_{21}(\tau) &= c_{12}(-\tau) \end{aligned} \quad (4.15)$$

and

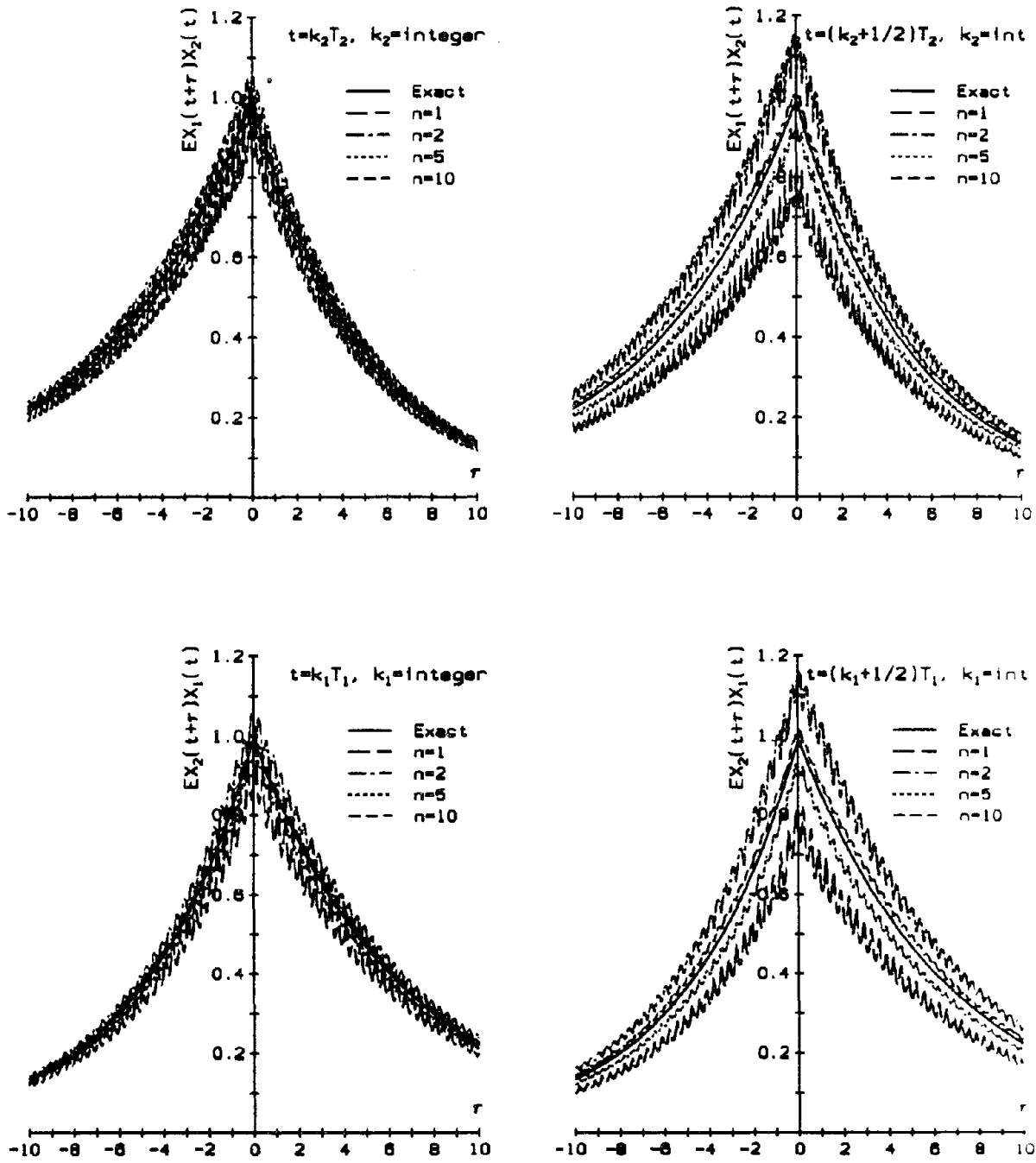
$$\begin{aligned} s_{rr}(f) &= \frac{1}{\rho_r^2 + (2\pi f)^2}, \quad r = 1, 2 \\ s_{12}(f) &= \frac{\rho_1 \rho_2 + (2\pi f)^2 + \sqrt{-1} (\rho_1 - \rho_2) 2\pi f}{[\rho_1 \rho_2 + (2\pi f)^2]^2 + [(\rho_1 - \rho_2) 2\pi f]^2} \end{aligned} \quad (4.16)$$

Figure 4-5 shows exact and approximate covariance functions of the stationary response $\underline{X}(t)$ in Eq. (4.14) for several values of ρ_r , $r = 1, 2$, and instances t coinciding with nodes and mid points between nodes. The approximate covariance functions are based on the local representation in Eq. (3.30) and window sizes $n = 1, 2, 5, 10$. The local representation in Eq. (3.30) is a



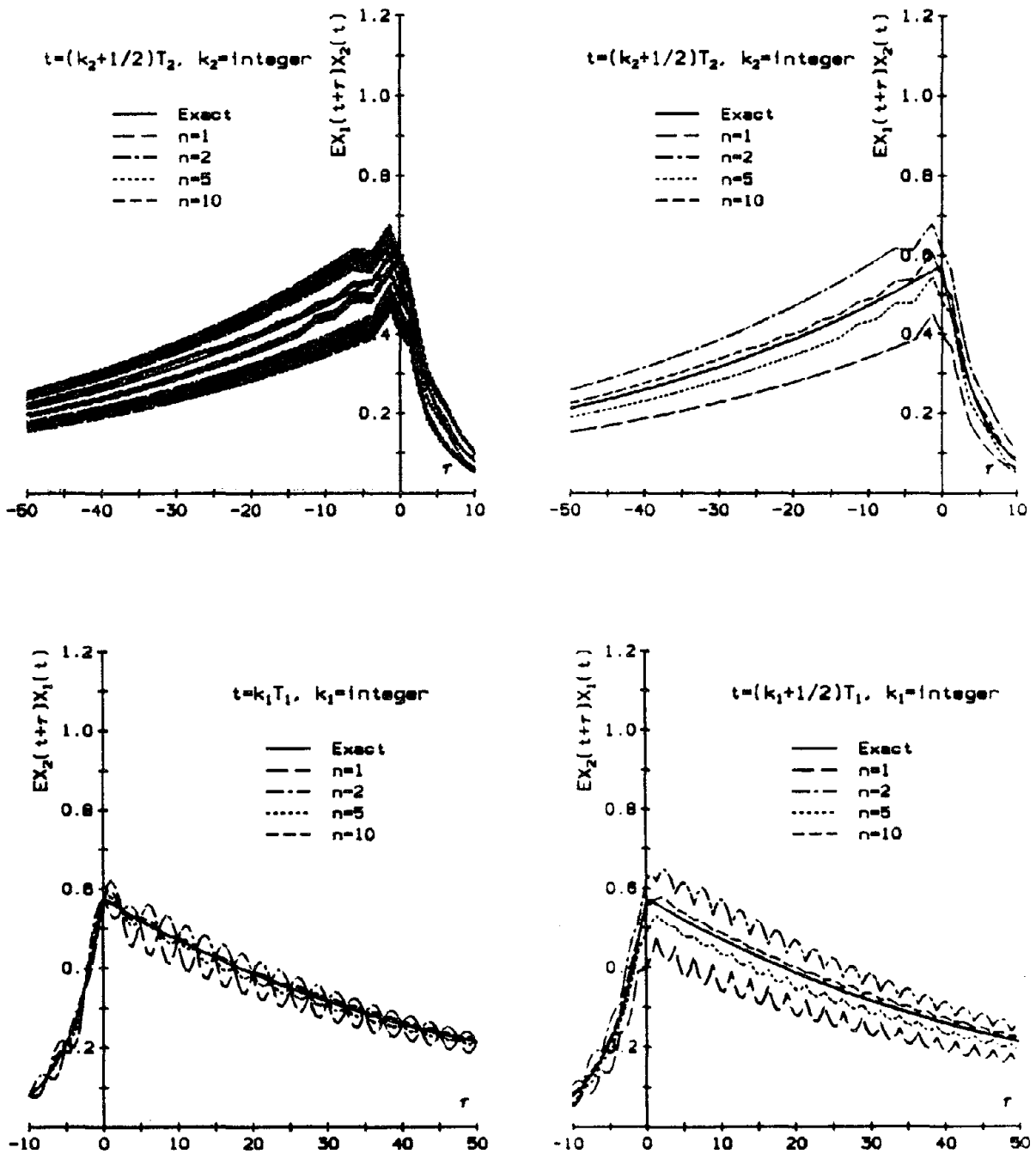
(a) $\rho_1 = 0.20, \rho_2 = 0.15$

FIGURE 4-5 Covariance functions of $\underline{Y}_n(t)$ in Eq. (3.30) and $\underline{X}(t)$ for the Bivariate Gaussian Process $\underline{X}(t)$ in Eq. (4.14)



(a) $\rho_1 = 0.20, \rho_2 = 0.15$

FIGURE 4-5 Covariance functions of $\underline{Y}_n(t)$ in Eq. (3.30) and $\underline{X}(t)$ for the Bivariate Gaussian Process $\underline{X}(t)$ in Eq. (4.14)



(b) $\rho_1 = 0.20, \rho_2 = 0.02$

FIGURE 4-5 Covariance functions of $\underline{Y}_n(t)$ in Eq. (3.30) and $\underline{X}(t)$ for the Bivariate Gaussian Process $\underline{X}(t)$ in Eq. (4.14)

nonstationary Gaussian process. However, the representation approaches $\underline{X}(t)$ as the window size n increases.

4.3. Random Fields ($q > 1, p = 1$)

Consider an argument \underline{t} , the corresponding cell $\prod_{s=1}^q [n_s(\underline{t})T_s, (n_s(\underline{t})+1)T_s]$, and the local representation $Y_{\underline{n}}(\underline{t})$ in Eq. (3.36) depending on the nodal values X_{k_1, \dots, k_q} , $k_s = n_s(\underline{t}) - n_s, \dots, n_s(\underline{t}) + n_s + 1$, $s = 1, \dots, q$. Consider also a rectangular domain $D = \prod_{s=1}^q [0, a_s]$ in R^q .

The objective is to generate samples of $X(\underline{t})$ in D based on the model $Y_{\underline{n}}(\underline{t})$ in Eq. (3.36). The case $q = 2$ is used to demonstrate the algorithm. Suppose first that $\bar{n}_1 \gg \bar{n}_2$, where $\bar{n}_s = a_s/T_s$, $s = 1, 2$, as shown in figure 4-6. Then, the model $Y_{\underline{n}}(\underline{t})$ can be given in the form

$$Y_{\underline{n}}(\underline{t}) = \sum_{k_1=n_1(\underline{t})-n_1}^{n_1(\underline{t})+n_1+1} X_{k_1}(t_2) \alpha_{k_1}(t_1; T_1) \quad (4.17)$$

in which

$$X_{k_1}(t_2) = \sum_{k_2=-n_2}^{n_2+\bar{n}_2+1} X_{k_1, k_2} \alpha_{k_2}(t_2; T_2) \quad (4.18)$$

The simulation of a realization of $X(\underline{t})$ in D can proceed in cycles generating realizations of the field in sets of cells, cells $1, \dots, \bar{n}_2$ in the first cycle, cells $\bar{n}_2+1, \dots, 2\bar{n}_2$ in the second cycle, and so on. The simulation starts with the generation of samples of $X(\underline{t})$ at nodal points $(k_1 T_1, k_2 T_2)$, $k_1 = -n_1, \dots, n_1+1$, $k_2 = -n_2, \dots, n_2+\bar{n}_2+1$. Then, Eqs. (4.17) and (4.18) can

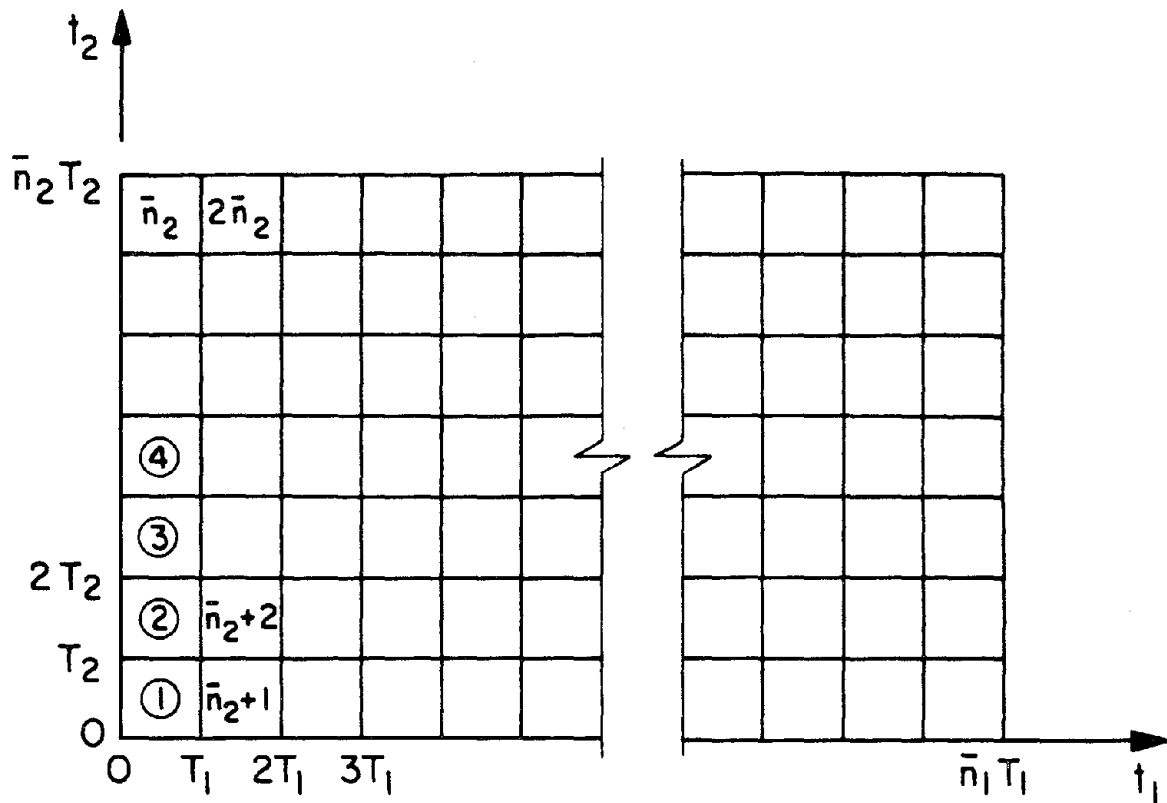


FIGURE 4-6 Domain $D = [0, a_1] \times [0, a_2] = [0, \bar{n}_1 T_1] \times [0, \bar{n}_2 T_2]$. Partition in Cells, Cell Numbers, and Nodal Points

be used to obtain a realization of $X(\underline{t})$ in cells $1, \dots, \bar{n}_2$. This completes the first cycle. The second cycle starts with the generation of samples of $X(\underline{t})$ at nodal points $(k_1 T_1, k_2 T_2)$, $k_1 = n_1 + 2, k_2 = -n_2, \dots, n_2 + \bar{n}_2 + 1$, that are needed to calculate $Y_{\underline{n}}(t)$ from Eqs. (4.17) and (4.18) when \underline{t} belongs to cells $\bar{n}_2 + 1, \dots, 2\bar{n}_2$. The nodal values of the field generated in this cycle are dependent on the previously generated nodal values of $X(\underline{t})$. The algorithm generates a sample of the conditional Gaussian vector $\underline{V}_2 = \{X((n_1 + 2)T_1, -n_2 T_2), \dots, X((n_1 + 2)T_1, (n_2 + \bar{n}_2 + 1)T_2)\}'$ given the values of vector $\underline{V} = \{X(k_1 T_1, k_2 T_2), k_1 = -n_1, \dots, n_1 + 1, k_2 = -n_2, \dots, n_2 + \bar{n}_2 + 1\}'$. These vectors have dimensions $2n_2 + \bar{n}_2 + 1$ and $2(n_1 + 1)(2n_2 + \bar{n}_2 + 1)$, respectively. All the subsequent cycles are similar to cycle 2. The generation of conditional Gaussian variables can be based on the algorithm in the Appendix.

The simulation procedure in Eqs. (4.17) and (4.18) becomes less satisfactory when both \bar{n}_1 and \bar{n}_2 are large because the number of random variables that has to be stored during every cycle increases substantially. Alternative simulation algorithms can be developed in this more general case. For example, Eq. (3.36) can be used directly to generate a sample of $X(\underline{t})$ by "marching" from cell to cell. The algorithm has to account for previously generated nodal values of $X(\underline{t})$ that may affect the sample of the field in any particular cell. The complexity of the simulation algorithm increases when the dimension of the field q exceeds 2 and/or the domain D is not rectangular. Nevertheless, the complexity relates to bookkeeping issues rather than conceptual or theoretical considerations.

Example 1. Consider a real-valued homogeneous Gaussian field $X(\underline{t})$ defined on R^2 with mean zero and power spectral density

$$s(\underline{f}) = \begin{cases} s_0 & , \quad \underline{f} \in (-\underline{f}_1, \underline{f}_1) \times (-\underline{f}_2, \underline{f}_2) \\ 0 & , \quad \text{otherwise} \end{cases} \quad (4.19)$$

where $s_0 = 1/(16 \pi^2 \underline{f}_1 \underline{f}_2)$ and $0 < \underline{f}_s < \infty$, $s = 1, 2$. The field has the covariance function

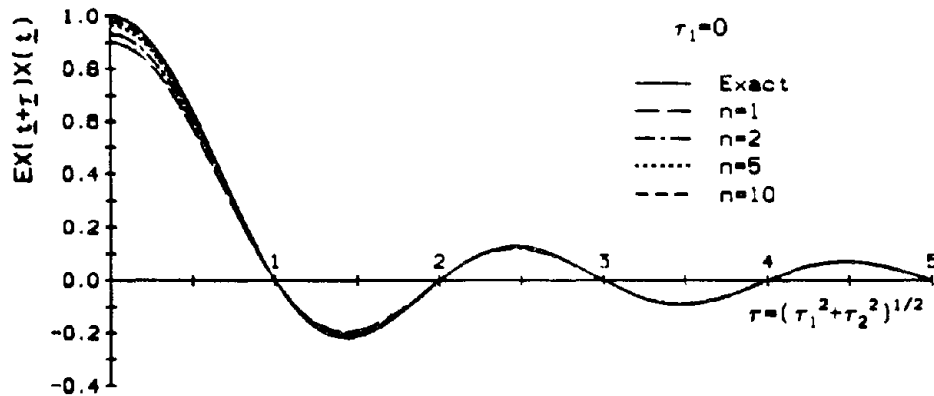
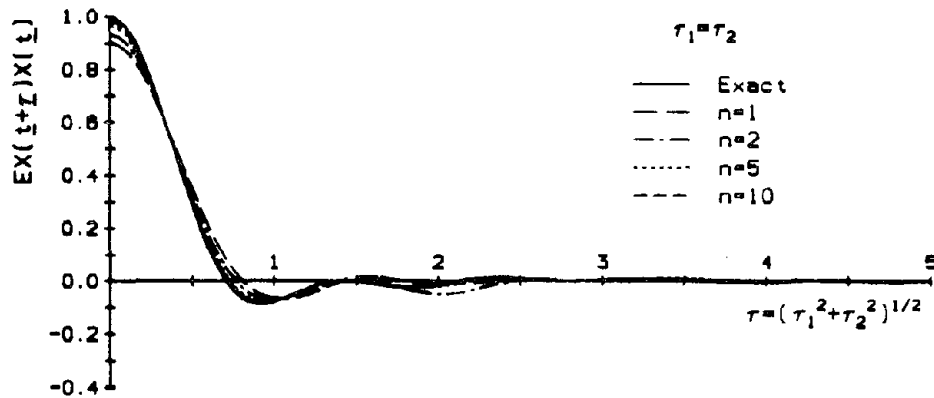
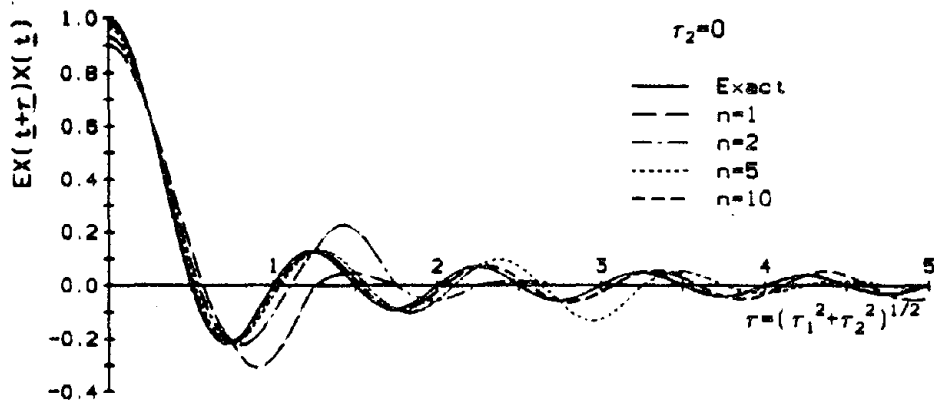
$$c(\underline{r}) = E X(\underline{t} + \underline{r}) X(\underline{t}) = \sigma^2 \prod_{s=1}^2 \frac{\sin(2\pi \underline{f}_s \tau_s)}{2\pi \underline{f}_s \tau_s} \quad (4.20)$$

and variance $c(\underline{0}) = 1$. It is referred to as band-limited Gaussian white noise random field.

The covariance function of two local representations of order \underline{m} and \underline{n} in Eq. (3.36) is

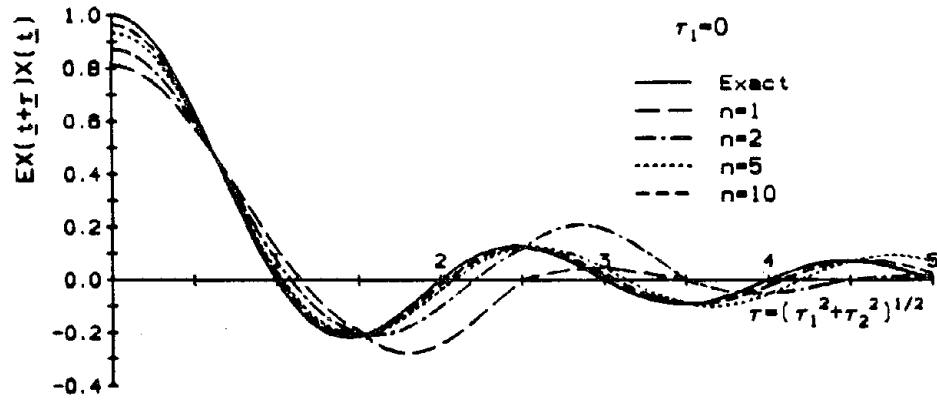
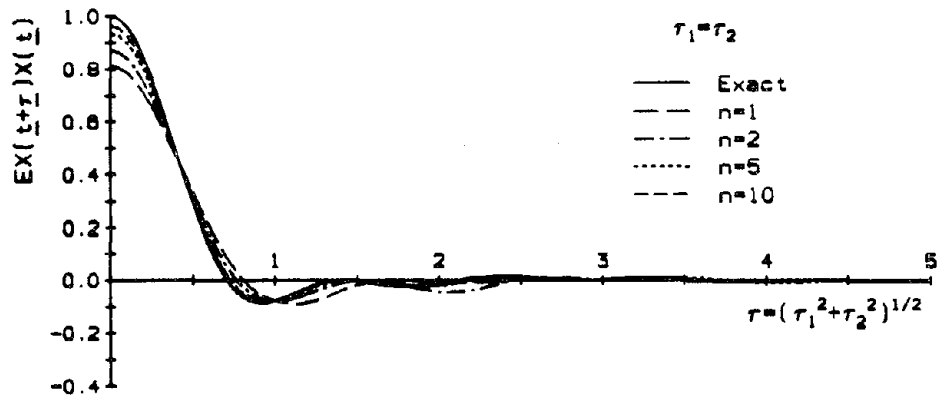
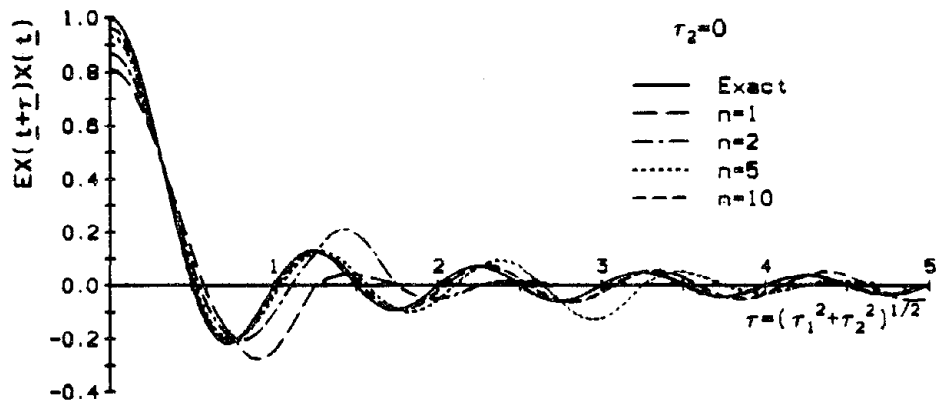
$$\begin{aligned} c_{\underline{n}, \underline{m}}(\underline{t} + \underline{r}, \underline{t}) &= E Y_{\underline{n}}(\underline{t} + \underline{r}) Y_{\underline{m}}(\underline{t}) \\ &= \sum_{k_1 = n_1(\underline{t} + \underline{r}) - n_1}^{n_1(\underline{t} + \underline{r}) + n_1 + 1} \sum_{k_2 = n_2(\underline{t} + \underline{r}) - n_2}^{n_2(\underline{t} + \underline{r}) + n_2 + 1} \sum_{\ell_1 = m_1(\underline{t}) - m_1}^{m_1(\underline{t}) + m_1 + 1} \sum_{\ell_2 = m_2(\underline{t}) - m_2}^{m_2(\underline{t}) + m_2 + 1} c((k_1 - \ell_1)T_1, (k_2 - \ell_2)T_2) \\ &\quad * \prod_{s=1}^2 \alpha_{k_s}(t_s + \tau_s; T_s) \prod_{u=1}^2 \alpha_{\ell_u}(t_u; T_u) \end{aligned} \quad (4.21)$$

Figure 4-7 shows exact and approximate covariance functions in Eqs. (4.20) and (4.21) for several values of \underline{t} , $\underline{m} = \underline{n}$, $\underline{f}_1 = 1.0$, and $\underline{f}_2 = 0.5$, as a function of the lag $\tau = (\tau_1^2 + \tau_2^2)^{1/2}$ for several values of τ_1 and τ_2 . The local representation $Y_{\underline{n}}(\underline{t})$ is not stationary, as previously indicated. However, it is nearly stationary unless the window size \underline{n} is extremely small. The figure does not show approximate covariances for \underline{t} equal to a nodal point because they coincide with the exact covariances for a band-limited white noise field.



(a) $t_1 = (k_1 + 1/2)T_1$, $t_2 = k_2T_2$, $k_s = \text{integer}$, $s = 1, 2$

FIGURE 4-7 Covariance Functions of $Y_n(\underline{t})$ in Eq. (3.36) and $X(\underline{t})$ for a Bivariate Band-Limited Gaussian White Noise Random Field



(b) $t_s = (k_s + 1/2)T_s$, $k_s = \text{integer}$, $s = 1, 2$

FIGURE 4-7 Covariance Functions of $Y_n(t)$ in Eq. (3.36) and $X(t)$ for a Bivariate Band-Limited Gaussian White Noise Random Field

Example 2. Consider a real-valued homogenous Gaussian random field $X(\underline{t})$, $\underline{t} \in R^2$, with zero-mean, unit-variance, power spectral density

$$s(\underline{f}) = \frac{1}{2\pi} \prod_{s=1}^2 \frac{d_s}{2\pi} \exp \left[- \frac{(d_s f_s)^2}{2} \right] \quad (4.22)$$

where $d_s > 0$, $s = 1, 2$, and covariance function

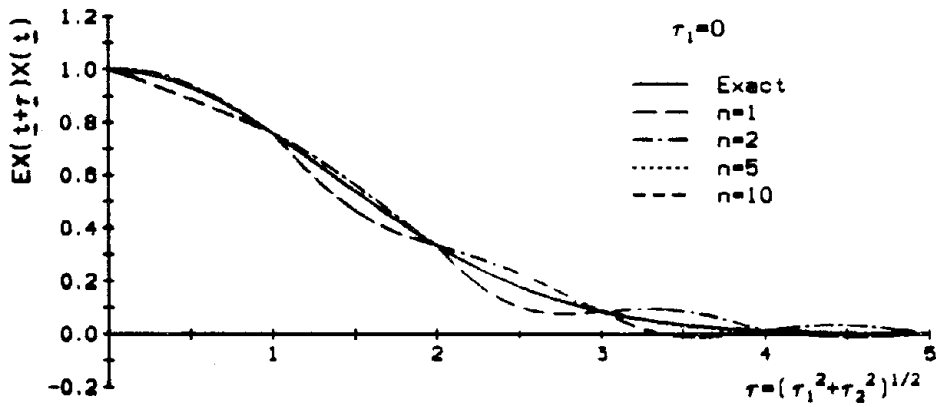
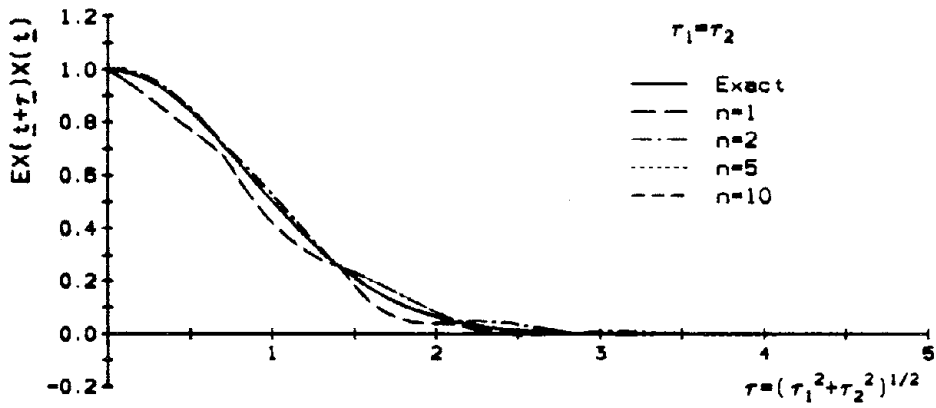
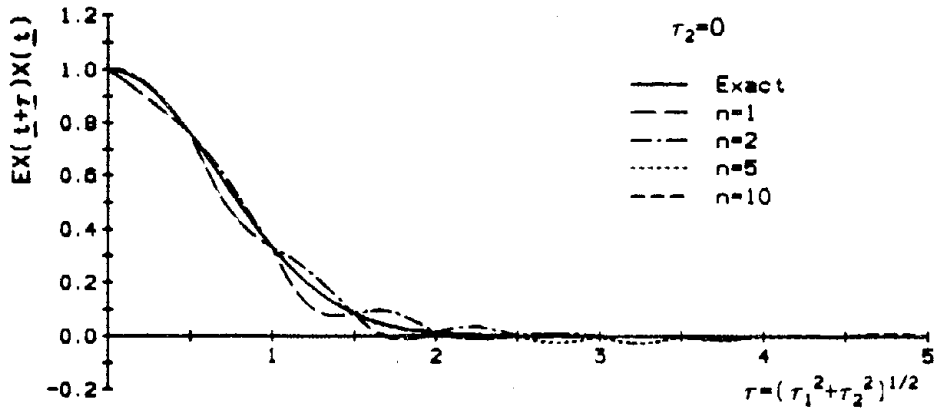
$$c(\underline{r}) = \exp \left[- \sum_{s=1}^2 \left[\frac{\pi r_s}{d_s} \right]^2 \right] \quad (4.23)$$

To apply the simulation algorithms, $s(\underline{f})$ is approximated by

$$\tilde{s}(\underline{f}) = \begin{cases} s(\underline{f}) & , \quad f_s = (-\bar{f}_s, \bar{f}_s) \quad , \quad s = 1, 2 \\ 0 & , \quad \text{otherwise} \end{cases} \quad (4.24)$$

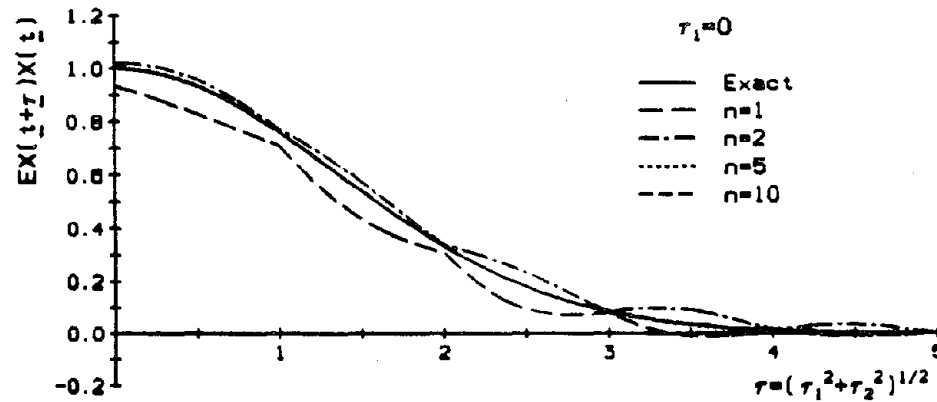
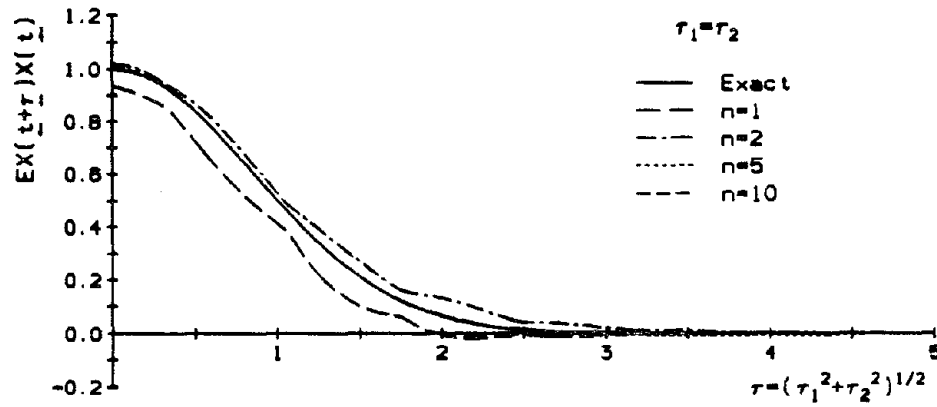
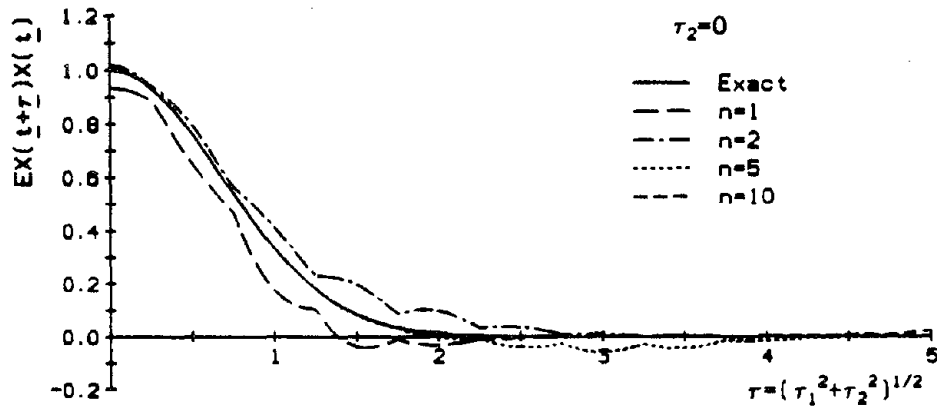
in which $0 < \bar{f}_s < \infty$, $s = 1, 2$, are so chosen that most of the power of $s(\underline{f})$ is included in $(-\bar{f}_1, \bar{f}_1) \times (-\bar{f}_2, \bar{f}_2)$.

Figure 4-8 shows exact and approximate covariance functions of the field. The approximate covariance functions are based on the local representation in Eq. (3.36), $\bar{f}_1 = 1.0$, $\bar{f}_2 = 0.5$, $d_1 = 3$, and $d_2 = 6$. Results show that the approximate covariance functions approach stationarity and the exact covariance functions as the window sizes increase.



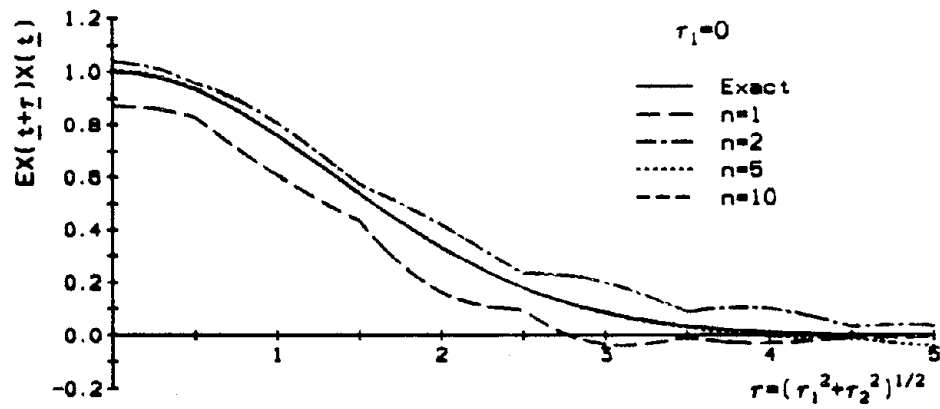
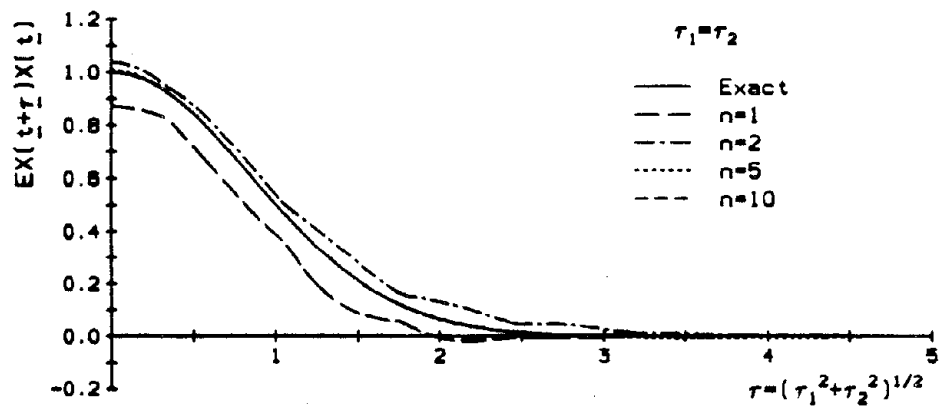
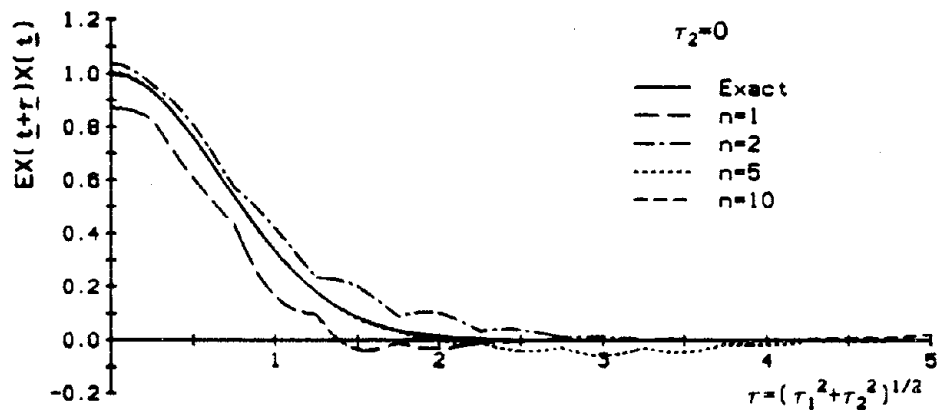
(a) $t_s = k_s T_s$, $k_s = \text{integer}$, $s = 1, 2$

FIGURE 4-8 Covariance Functions of $Y_n(t)$ in Eq. (3.36) and $X(t)$ for a Bivariate Random Field with Truncated Gaussian Spectrum



(b) $t_1 = (k_1 + 1/2)T_s$, $t_2 = k_2T_2$, $k_s = \text{integer}$, $s = 1, 2$

FIGURE 4-8 Covariance Functions of $Y_n(\underline{t})$ in Eq. (3.36) and $X(\underline{t})$ for a Bivariate Random Field with Truncated Gaussian Spectrum



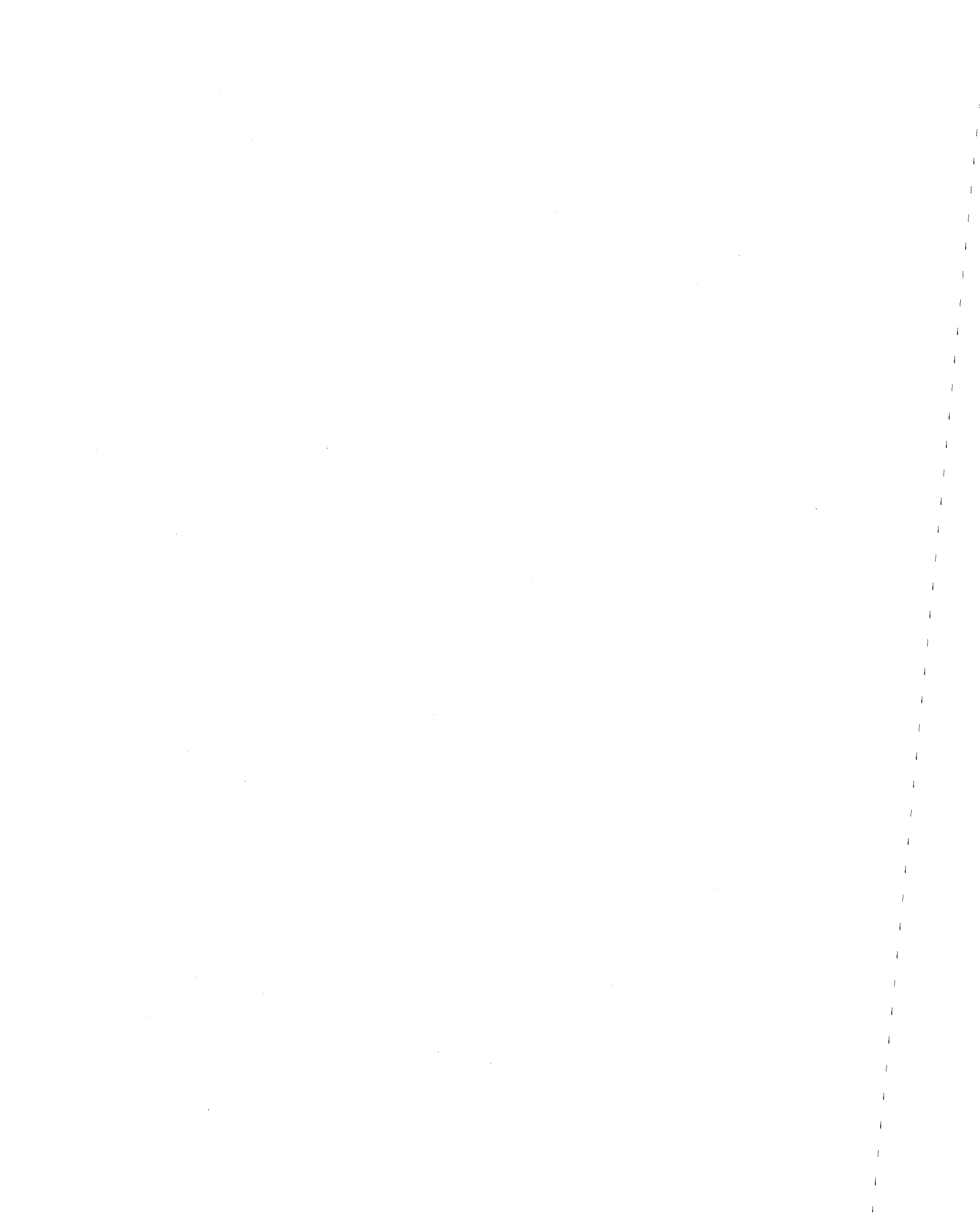
(c) $t_s = (k_s + 1/2)T_s$, $k_s = \text{integer}$, $s = 1, 2$

FIGURE 4-8 Covariance Functions of $Y_n(t)$ in Eq. (3.36) and $X(t)$ for a Bivariate Random Field with Truncated Gaussian Spectrum

SECTION 5 CONCLUSIONS

A general method was developed for generating samples of stationary Gaussian processes, vector processes, fields, and vector fields. The method is based on the sampling theorem for real-valued deterministic and random functions defined on the real line and a generalization of it for vector functions defined on vector spaces. The probabilistic model of a stationary Gaussian random function used in simulation depends on a finite number of values of this function at a set of points, referred as nodes. The model (i) improves as the number of nodes increases; (ii) converges to the random function as the number of nodes approaches infinity; (iii) is simple; and (iv) is fully defined by the finite dimensional distributions of the random function. Moreover, the algorithm is efficient and sample generation can be performed online, analogous to the generation by the ARMA sequence. The codification of the simulation algorithm can be delicate for vector random processes and fields because of bookkeeping issues.

Several examples were presented to illustrate the simulation method and evaluate the rate of convergence of the proposed probabilistic models to the random functions they represent. The examples include random processes, vector random processes, and random fields. Numerical results demonstrate that the proposed simulation method is a viable alternative to current techniques for the generation of realizations of stationary Gaussian functions.



SECTION 6
REFERENCES

1. Adler, R. I., The Geometry of Random Fields, John Wiley & Sons, New York, 1981.
2. Brigham, E. O., The Fast Fourier Transform, Prentice-Hall, Inc., Englewood Cliffs, New Jersey, 1974.
3. Cramer, H. and Leadbetter, M. R., Stationary and Related Processes, John Wiley & Sons, New York, 1967.
4. Davenport, W. B., and Root, W. L., An Introduction to the Theory of Random Signals and Noise, McGraw-Hill Book Co., Inc., New York, 1958.
5. Deodatis, G. and Shinozuka, M., "Auto-Regressive Model for Nonstationary Stochastic Processes," Journal of Engineering Mechanics, Vol. 114, No. 11, November 1988, pp. 1995-2012.
6. Grigoriu, M., "Crossings of Non-Gaussian Translation Processes," Journal of Engineering Mechanics, ASCE, Vol. 110, No. EM4, April 1984, pp. 610-620.
7. Grigoriu, M., Ruiz, S. E., and Rosenblueth, E., "Nonstationary Models of Seismic Ground Acceleration," Earthquake Spectra, The Professional Journal of Earthquake Engineering Research Institute, Vol. 4, No. 3, August 1988, pp. 551-568.
8. Kozin, F., "Autoregressive Moving Average Models of Earthquake Records," Probabilistic Engineering Mechanics, Vol. 3, No. 2, June 1988, pp. 58-63.
9. Rubinstein, R. Y., Simulation and the Monte Carlo Method, John Wiley & Sons, New York, 1981.
10. Samaras, E., Shinozuka, M., and Tsurui, A., "ARMA Representation of Random Processes," Journal of Engineering Mechanics, ASCE, Vol. 111, No. 3, pp. 449-461.
11. Shinozuka, M. and Sato, Y., "Simulation of Nonstationary Random Processes," Journal of Engineering Mechanics, ASCE, 93, EM 1, February 1967, pp. 11-40.
12. Shinozuka, M., "Simulation of Multivariate and Multidimensional Random Processes," The Journal of the Acoustical Society of America, Vol. 49, No. 1 (Part 2), 1971, pp. 357-367.
13. Shinozuka, M. and Jan, C.-M., "Digital Simulation of Random Processes and its Applications," Journal of Sound and Vibration, Vol. 25, No. 1, 1977, pp. 111-128.
14. Shinozuka, M., "Stochastic Fields and Their Digital Simulation," Stochastic Methods in Structural Dynamics, G. I. Schüeller and M. Shinozuka, eds, Martinus Nijhoff Publishers, Boston, 1987, pp. 93-133.

15. Shinozuka, M. and Deodatis, G., "Simulation of Stochastic Processes by Spectral Representation," Applied Mechanics Reviews, Vol. 44, No. 4, April 1991, pp. 191-203.
16. Spanos, P. D., "ARMA Algorithms for Ocean Wave Modeling," Journal of Energy Resources Technology, Trans. of ASME, Vol. 105, 1983, pp. 681-687.
17. Veneziano, D., Grigoriu, M., and Cornell, C. A., "Vector-Process Models for System Reliability," Journal of the Engineering Mechanics Division, ASCE, Vol. 103, No. EM3, June 1977, pp. 441-460.
18. Wong, E. and Hajek, B., Stochastic Processes in Engineering Systems, Springer Verlag, New York, 1985.
19. Yamazaki, F. and Shinozuka, M., "Digital Generation of the Non-Gaussian Stochastic Fields," Stochastic Mechanics, Vol. I, ed. M. Shinozuka, Columbia University, New York, June 1987, pp. 209-211.

**APPENDIX
GENERATION OF CONDITIONAL GAUSSIAN VARIABLES AND VECTORS**

Let \underline{Y} be a n -dimensional zero-mean Gaussian vector with covariances $\gamma_{k\ell} = EY_k Y_\ell$, $k, \ell = 1, \dots, n$. Consider a partition of \underline{Y} in two vectors $\underline{Y}^{(1)}$ and $\underline{Y}^{(2)}$ consisting of the first $1 \leq n_1 < n$ and the last $n_2 = n - n_1$ components of \underline{Y} . Suppose that a value $y^{(1)}$ of $\underline{Y}^{(1)}$ is given. The objective is to generate samples of the conditional Gaussian vector $\hat{\underline{Y}}^{(2)} = \underline{Y}^{(2)} \mid \underline{Y}^{(1)} = y^{(1)}$. Consider the transformation [9]

$$\underline{Y} = \underline{a} \underline{V} \tag{A.1}$$

in which \underline{V} is a vector consisting of n independent standard Gaussian variables with zero mean and unit variance and \underline{a} is a lower triangular matrix with components

$$a_{k\ell} = \frac{\gamma_{k\ell} - \sum_{j=1}^{\ell-1} a_{kj} a_{\ell j}}{\left[\gamma_{k\ell} - \sum_{j=1}^{\ell-1} a_{\ell j}^2 \right]^{1/2}}, \quad k = 1, 2, \dots, n; \quad 1 \leq \ell \leq k \tag{A.2}$$

and the convention $\sum_{j=1}^0 a_{kj} a_{\ell j} = \sum_{j=1}^0 a_{\ell j}^2 = 0$. The determination of matrix \underline{a} can be performed sequentially starting with the first row and involves elementary algebraic calculations. Moreover, the components of \underline{V} can be obtained from the components of \underline{Y} sequentially, and the equalities

$$v_k = \frac{1}{a_{kk}} \left[Y_k - \sum_{\ell=1}^{k-1} a_{k\ell} v_\ell \right], \quad k = 1, 2, 3, \dots, n \tag{A.3}$$

with the starting condition $v_1 = \frac{1}{a_{11}} Y_1$.

Suppose that $\underline{Y}^{(1)} = \underline{y}^{(1)} = (y_1, \dots, y_{n_1})$. From Eq. (A.3), the first n_1 components of \underline{V} are equal to

$$v_k = \frac{1}{a_{kk}} \left[y_k - \sum_{\ell=1}^{k-1} a_{k\ell} v_\ell \right], \quad k = 2, \dots, n_1 \quad (\text{A.4})$$

in which $v_1 = \frac{1}{a_{11}} y_1$. Let $\underline{v}^{(1)} = (v_1, \dots, v_{n_1})'$ be a vector consisting of components calculated in Eq. (A.4) and $\underline{v}^{(2)}$ a vector of n_2 independent standard variables. Then, from Eq. (A.1), the conditional vector $\hat{\underline{Y}}^{(2)}$ is

$$\hat{\underline{Y}}^{(2)} = \underline{a}_{21} \underline{v}^{(1)} + \underline{a}_{22} \underline{v}^{(2)} \quad (\text{A.5})$$

in which \underline{a}_{21} consists of the last n_2 rows and the first n_1 columns of \underline{a} while \underline{a}_{22} is a n_2 -dimensional lower triangular square matrix obtained from the last n_2 rows and columns of \underline{a} .

The generation of samples of $\hat{\underline{Y}}^{(2)}$ is based on Eq. (A.5). It involves generation of a realization $\underline{v}^{(2)}$ of the n_2 independent standard Gaussian variables $\underline{v}^{(2)}$ and calculation of the corresponding value $\hat{\underline{Y}}^{(2)}$ of the conditional vector $\hat{\underline{Y}}^{(2)} = \underline{Y}^{(2)} | \underline{Y}^{(1)} = \underline{y}^{(1)}$ from Eq. A.5,

$$\hat{\underline{Y}}^{(2)} = \underline{a}_{21} \underline{v}^{(1)} + \underline{a}_{22} \underline{v}^{(2)} \quad (\text{A.6})$$

**NATIONAL CENTER FOR EARTHQUAKE ENGINEERING RESEARCH
LIST OF TECHNICAL REPORTS**

The National Center for Earthquake Engineering Research (NCEER) publishes technical reports on a variety of subjects related to earthquake engineering written by authors funded through NCEER. These reports are available from both NCEER's Publications Department and the National Technical Information Service (NTIS). Requests for reports should be directed to the Publications Department, National Center for Earthquake Engineering Research, State University of New York at Buffalo, Red Jacket Quadrangle, Buffalo, New York 14261. Reports can also be requested through NTIS, 5285 Port Royal Road, Springfield, Virginia 22161. NTIS accession numbers are shown in parenthesis, if available.

- NCEER-87-0001 "First-Year Program in Research, Education and Technology Transfer," 3/5/87, (PB88-134275/AS).
- NCEER-87-0002 "Experimental Evaluation of Instantaneous Optimal Algorithms for Structural Control," by R.C. Lin, T.T. Soong and A.M. Reinhorn, 4/20/87, (PB88-134341/AS).
- NCEER-87-0003 "Experimentation Using the Earthquake Simulation Facilities at University at Buffalo," by A.M. Reinhorn and R.L. Ketter, to be published.
- NCEER-87-0004 "The System Characteristics and Performance of a Shaking Table," by J.S. Hwang, K.C. Chang and G.C. Lee, 6/1/87, (PB88-134259/AS). This report is available only through NTIS (see address given above).
- NCEER-87-0005 "A Finite Element Formulation for Nonlinear Viscoplastic Material Using a Q Model," by O. Gyebi and G. Dasgupta, 11/2/87, (PB88-213764/AS).
- NCEER-87-0006 "Symbolic Manipulation Program (SMP) - Algebraic Codes for Two and Three Dimensional Finite Element Formulations," by X. Lee and G. Dasgupta, 11/9/87, (PB88-219522/AS).
- NCEER-87-0007 "Instantaneous Optimal Control Laws for Tall Buildings Under Seismic Excitations," by J.N. Yang, A. Akbarpour and P. Ghaemmaghami, 6/10/87, (PB88-134333/AS).
- NCEER-87-0008 "IDARC: Inelastic Damage Analysis of Reinforced Concrete Frame - Shear-Wall Structures," by Y.J. Park, A.M. Reinhorn and S.K. Kunnath, 7/20/87, (PB88-134325/AS).
- NCEER-87-0009 "Liquefaction Potential for New York State: A Preliminary Report on Sites in Manhattan and Buffalo," by M. Budhu, V. Vijayakumar, R.F. Giese and L. Baumgras, 8/31/87, (PB88-163704/AS). This report is available only through NTIS (see address given above).
- NCEER-87-0010 "Vertical and Torsional Vibration of Foundations in Inhomogeneous Media," by A.S. Veletsos and K.W. Dotson, 6/1/87, (PB88-134291/AS).
- NCEER-87-0011 "Seismic Probabilistic Risk Assessment and Seismic Margins Studies for Nuclear Power Plants," by Howard H.M. Hwang, 6/15/87, (PB88-134267/AS).
- NCEER-87-0012 "Parametric Studies of Frequency Response of Secondary Systems Under Ground-Acceleration Excitations," by Y. Yong and Y.K. Lin, 6/10/87, (PB88-134309/AS).
- NCEER-87-0013 "Frequency Response of Secondary Systems Under Seismic Excitation," by J.A. HoLung, J. Cai and Y.K. Lin, 7/31/87, (PB88-134317/AS).
- NCEER-87-0014 "Modelling Earthquake Ground Motions in Seismically Active Regions Using Parametric Time Series Methods," by G.W. Ellis and A.S. Cakmak, 8/25/87, (PB88-134283/AS).
- NCEER-87-0015 "Detection and Assessment of Seismic Structural Damage," by E. DiPasquale and A.S. Cakmak, 8/25/87, (PB88-163712/AS).

- NCEER-87-0016 "Pipeline Experiment at Parkfield, California," by J. Isenberg and E. Richardson, 9/15/87, (PB88-163720/AS). This report is available only through NTIS (see address given above).
- NCEER-87-0017 "Digital Simulation of Seismic Ground Motion," by M. Shinozuka, G. Deodatis and T. Harada, 8/31/87, (PB88-155197/AS). This report is available only through NTIS (see address given above).
- NCEER-87-0018 "Practical Considerations for Structural Control: System Uncertainty, System Time Delay and Truncation of Small Control Forces," J.N. Yang and A. Akbarpour, 8/10/87, (PB88-163738/AS).
- NCEER-87-0019 "Modal Analysis of Nonclassically Damped Structural Systems Using Canonical Transformation," by J.N. Yang, S. Sarkani and F.X. Long, 9/27/87, (PB88-187851/AS).
- NCEER-87-0020 "A Nonstationary Solution in Random Vibration Theory," by J.R. Red-Horse and P.D. Spanos, 11/3/87, (PB88-163746/AS).
- NCEER-87-0021 "Horizontal Impedances for Radially Inhomogeneous Viscoelastic Soil Layers," by A.S. Veletsos and K.W. Dotson, 10/15/87, (PB88-150859/AS).
- NCEER-87-0022 "Seismic Damage Assessment of Reinforced Concrete Members," by Y.S. Chung, C. Meyer and M. Shinozuka, 10/9/87, (PB88-150867/AS). This report is available only through NTIS (see address given above).
- NCEER-87-0023 "Active Structural Control in Civil Engineering," by T.T. Soong, 11/11/87, (PB88-187778/AS).
- NCEER-87-0024 "Vertical and Torsional Impedances for Radially Inhomogeneous Viscoelastic Soil Layers," by K.W. Dotson and A.S. Veletsos, 12/87, (PB88-187786/AS).
- NCEER-87-0025 "Proceedings from the Symposium on Seismic Hazards, Ground Motions, Soil-Liquefaction and Engineering Practice in Eastern North America," October 20-22, 1987, edited by K.H. Jacob, 12/87, (PB88-188115/AS).
- NCEER-87-0026 "Report on the Whittier-Narrows, California, Earthquake of October 1, 1987," by J. Pantelic and A. Reinhorn, 11/87, (PB88-187752/AS). This report is available only through NTIS (see address given above).
- NCEER-87-0027 "Design of a Modular Program for Transient Nonlinear Analysis of Large 3-D Building Structures," by S. Srivastav and J.F. Abel, 12/30/87, (PB88-187950/AS).
- NCEER-87-0028 "Second-Year Program in Research, Education and Technology Transfer," 3/8/88, (PB88-219480/AS).
- NCEER-88-0001 "Workshop on Seismic Computer Analysis and Design of Buildings With Interactive Graphics," by W. McGuire, J.F. Abel and C.H. Conley, 1/18/88, (PB88-187760/AS).
- NCEER-88-0002 "Optimal Control of Nonlinear Flexible Structures," by J.N. Yang, F.X. Long and D. Wong, 1/22/88, (PB88-213772/AS).
- NCEER-88-0003 "Substructuring Techniques in the Time Domain for Primary-Secondary Structural Systems," by G.D. Manolis and G. Juhn, 2/10/88, (PB88-213780/AS).
- NCEER-88-0004 "Iterative Seismic Analysis of Primary-Secondary Systems," by A. Singhal, L.D. Lutes and P.D. Spanos, 2/23/88, (PB88-213798/AS).
- NCEER-88-0005 "Stochastic Finite Element Expansion for Random Media," by P.D. Spanos and R. Ghanem, 3/14/88, (PB88-213806/AS).

- NCEER-88-0006 "Combining Structural Optimization and Structural Control," by F.Y. Cheng and C.P. Pantelides, 1/10/88, (PB88-213814/AS).
- NCEER-88-0007 "Seismic Performance Assessment of Code-Designed Structures," by H.H-M. Hwang, J-W. Jaw and H-J. Shau, 3/20/88, (PB88-219423/AS).
- NCEER-88-0008 "Reliability Analysis of Code-Designed Structures Under Natural Hazards," by H.H-M. Hwang, H. Ushiba and M. Shinozuka, 2/29/88, (PB88-229471/AS).
- NCEER-88-0009 "Seismic Fragility Analysis of Shear Wall Structures," by J-W Jaw and H.H-M. Hwang, 4/30/88, (PB89-102867/AS).
- NCEER-88-0010 "Base Isolation of a Multi-Story Building Under a Harmonic Ground Motion - A Comparison of Performances of Various Systems," by F-G Fan, G. Ahmadi and I.G. Tadjbakhsh, 5/18/88, (PB89-122238/AS).
- NCEER-88-0011 "Seismic Floor Response Spectra for a Combined System by Green's Functions," by F.M. Lavelle, L.A. Bergman and P.D. Spanos, 5/1/88, (PB89-102875/AS).
- NCEER-88-0012 "A New Solution Technique for Randomly Excited Hysteretic Structures," by G.Q. Cai and Y.K. Lin, 5/16/88, (PB89-102883/AS).
- NCEER-88-0013 "A Study of Radiation Damping and Soil-Structure Interaction Effects in the Centrifuge," by K. Weissman, supervised by J.H. Prevost, 5/24/88, (PB89-144703/AS).
- NCEER-88-0014 "Parameter Identification and Implementation of a Kinematic Plasticity Model for Frictional Soils," by J.H. Prevost and D.V. Griffiths, to be published.
- NCEER-88-0015 "Two- and Three- Dimensional Dynamic Finite Element Analyses of the Long Valley Dam," by D.V. Griffiths and J.H. Prevost, 6/17/88, (PB89-144711/AS).
- NCEER-88-0016 "Damage Assessment of Reinforced Concrete Structures in Eastern United States," by A.M. Reinhorn, M.J. Seidel, S.K. Kunnath and Y.J. Park, 6/15/88, (PB89-122220/AS).
- NCEER-88-0017 "Dynamic Compliance of Vertically Loaded Strip Foundations in Multilayered Viscoelastic Soils," by S. Ahmad and A.S.M. Israil, 6/17/88, (PB89-102891/AS).
- NCEER-88-0018 "An Experimental Study of Seismic Structural Response With Added Viscoelastic Dampers," by R.C. Lin, Z. Liang, T.T. Soong and R.H. Zhang, 6/30/88, (PB89-122212/AS). This report is available only through NTIS (see address given above).
- NCEER-88-0019 "Experimental Investigation of Primary - Secondary System Interaction," by G.D. Manolis, G. Juhn and A.M. Reinhorn, 5/27/88, (PB89-122204/AS).
- NCEER-88-0020 "A Response Spectrum Approach For Analysis of Nonclassically Damped Structures," by J.N. Yang, S. Sarkani and F.X. Long, 4/22/88, (PB89-102909/AS).
- NCEER-88-0021 "Seismic Interaction of Structures and Soils: Stochastic Approach," by A.S. Veletsos and A.M. Prasad, 7/21/88, (PB89-122196/AS).
- NCEER-88-0022 "Identification of the Serviceability Limit State and Detection of Seismic Structural Damage," by E. DiPasquale and A.S. Cakmak, 6/15/88, (PB89-122188/AS). This report is available only through NTIS (see address given above).
- NCEER-88-0023 "Multi-Hazard Risk Analysis: Case of a Simple Offshore Structure," by B.K. Bhartia and E.H. Vanmarcke, 7/21/88, (PB89-145213/AS).

- NCEER-88-0024 "Automated Seismic Design of Reinforced Concrete Buildings," by Y.S. Chung, C. Meyer and M. Shinozuka, 7/5/88, (PB89-122170/AS). This report is available only through NTIS (see address given above).
- NCEER-88-0025 "Experimental Study of Active Control of MDOF Structures Under Seismic Excitations," by L.L. Chung, R.C. Lin, T.T. Soong and A.M. Reinhorn, 7/10/88, (PB89-122600/AS).
- NCEER-88-0026 "Earthquake Simulation Tests of a Low-Rise Metal Structure," by J.S. Hwang, K.C. Chang, G.C. Lee and R.L. Ketter, 8/1/88, (PB89-102917/AS).
- NCEER-88-0027 "Systems Study of Urban Response and Reconstruction Due to Catastrophic Earthquakes," by F. Kozin and H.K. Zhou, 9/22/88, (PB90-162348/AS).
- NCEER-88-0028 "Seismic Fragility Analysis of Plane Frame Structures," by H.H.-M. Hwang and Y.K. Low, 7/31/88, (PB89-131445/AS).
- NCEER-88-0029 "Response Analysis of Stochastic Structures," by A. Kardara, C. Bucher and M. Shinozuka, 9/22/88, (PB89-174429/AS).
- NCEER-88-0030 "Nonnormal Accelerations Due to Yielding in a Primary Structure," by D.C.K. Chen and L.D. Lutes, 9/19/88, (PB89-131437/AS).
- NCEER-88-0031 "Design Approaches for Soil-Structure Interaction," by A.S. Veletsos, A.M. Prasad and Y. Tang, 12/30/88, (PB89-174437/AS). This report is available only through NTIS (see address given above).
- NCEER-88-0032 "A Re-evaluation of Design Spectra for Seismic Damage Control," by C.J. Turkstra and A.G. Tallin, 11/7/88, (PB89-145221/AS).
- NCEER-88-0033 "The Behavior and Design of Noncontact Lap Splices Subjected to Repeated Inelastic Tensile Loading," by V.E. Sagan, P. Gergely and R.N. White, 12/8/88, (PB89-163737/AS).
- NCEER-88-0034 "Seismic Response of Pile Foundations," by S.M. Mamoon, P.K. Banerjee and S. Ahmad, 11/1/88, (PB89-145239/AS).
- NCEER-88-0035 "Modeling of R/C Building Structures With Flexible Floor Diaphragms (IDARC2)," by A.M. Reinhorn, S.K. Kunnath and N. Panahshahi, 9/7/88, (PB89-207153/AS).
- NCEER-88-0036 "Solution of the Dam-Reservoir Interaction Problem Using a Combination of FEM, BEM with Particular Integrals, Modal Analysis, and Substructuring," by C-S. Tsai, G.C. Lee and R.L. Ketter, 12/31/88, (PB89-207146/AS).
- NCEER-88-0037 "Optimal Placement of Actuators for Structural Control," by F.Y. Cheng and C.P. Pantelides, 8/15/88, (PB89-162846/AS).
- NCEER-88-0038 "Teflon Bearings in Aseismic Base Isolation: Experimental Studies and Mathematical Modeling," by A. Mokha, M.C. Constantinou and A.M. Reinhorn, 12/5/88, (PB89-218457/AS). This report is available only through NTIS (see address given above).
- NCEER-88-0039 "Seismic Behavior of Flat Slab High-Rise Buildings in the New York City Area," by P. Weidlinger and M. Ettouney, 10/15/88, (PB90-145681/AS).
- NCEER-88-0040 "Evaluation of the Earthquake Resistance of Existing Buildings in New York City," by P. Weidlinger and M. Ettouney, 10/15/88, to be published.
- NCEER-88-0041 "Small-Scale Modeling Techniques for Reinforced Concrete Structures Subjected to Seismic Loads," by W. Kim, A. El-Attar and R.N. White, 11/22/88, (PB89-189625/AS).

- NCEER-88-0042 "Modeling Strong Ground Motion from Multiple Event Earthquakes," by G.W. Ellis and A.S. Cakmak, 10/15/88, (PB89-174445/AS).
- NCEER-88-0043 "Nonstationary Models of Seismic Ground Acceleration," by M. Grigoriu, S.E. Ruiz and E. Rosenbluth, 7/15/88, (PB89-189617/AS).
- NCEER-88-0044 "SARCF User's Guide: Seismic Analysis of Reinforced Concrete Frames," by Y.S. Chung, C. Meyer and M. Shinozuka, 11/9/88, (PB89-174452/AS).
- NCEER-88-0045 "First Expert Panel Meeting on Disaster Research and Planning," edited by J. Pantelic and J. Stoyke, 9/15/88, (PB89-174460/AS).
- NCEER-88-0046 "Preliminary Studies of the Effect of Degrading Infill Walls on the Nonlinear Seismic Response of Steel Frames," by C.Z. Chrysostomou, P. Gergely and J.F. Abel, 12/19/88, (PB89-208383/AS).
- NCEER-88-0047 "Reinforced Concrete Frame Component Testing Facility - Design, Construction, Instrumentation and Operation," by S.P. Pessiki, C. Conley, T. Bond, P. Gergely and R.N. White, 12/16/88, (PB89-174478/AS).
- NCEER-89-0001 "Effects of Protective Cushion and Soil Compliancy on the Response of Equipment Within a Seismically Excited Building," by J.A. HoLung, 2/16/89, (PB89-207179/AS).
- NCEER-89-0002 "Statistical Evaluation of Response Modification Factors for Reinforced Concrete Structures," by H.H.M. Hwang and J-W. Jaw, 2/17/89, (PB89-207187/AS).
- NCEER-89-0003 "Hysteretic Columns Under Random Excitation," by G-Q. Cai and Y.K. Lin, 1/9/89, (PB89-196513/AS).
- NCEER-89-0004 "Experimental Study of 'Elephant Foot Bulge' Instability of Thin-Walled Metal Tanks," by Z-H. Jia and R.L. Ketter, 2/22/89, (PB89-207195/AS).
- NCEER-89-0005 "Experiment on Performance of Buried Pipelines Across San Andreas Fault," by J. Isenberg, E. Richardson and T.D. O'Rourke, 3/10/89, (PB89-218440/AS).
- NCEER-89-0006 "A Knowledge-Based Approach to Structural Design of Earthquake-Resistant Buildings," by M. Subramani, P. Gergely, C.H. Conley, J.F. Abel and A.H. Zaghaw, 1/15/89, (PB89-218465/AS).
- NCEER-89-0007 "Liquefaction Hazards and Their Effects on Buried Pipelines," by T.D. O'Rourke and P.A. Lane, 2/1/89, (PB89-218481).
- NCEER-89-0008 "Fundamentals of System Identification in Structural Dynamics," by H. Imai, C-B. Yun, O. Maruyama and M. Shinozuka, 1/26/89, (PB89-207211/AS).
- NCEER-89-0009 "Effects of the 1985 Michoacan Earthquake on Water Systems and Other Buried Lifelines in Mexico," by A.G. Ayala and M.J. O'Rourke, 3/8/89, (PB89-207229/AS).
- NCEER-89-R010 "NCEER Bibliography of Earthquake Education Materials," by K.E.K. Ross, Second Revision, 9/1/89, (PB90-125352/AS).
- NCEER-89-0011 "Inelastic Three-Dimensional Response Analysis of Reinforced Concrete Building Structures (IDARC-3D), Part I - Modeling," by S.K. Kunnath and A.M. Reinhorn, 4/17/89, (PB90-114612/AS).
- NCEER-89-0012 "Recommended Modifications to ATC-14," by C.D. Poland and J.O. Malley, 4/12/89, (PB90-108648/AS).
- NCEER-89-0013 "Repair and Strengthening of Beam-to-Column Connections Subjected to Earthquake Loading," by M. Corazao and A.J. Durrani, 2/28/89, (PB90-109885/AS).

- NCEER-89-0014 "Program EXKAL2 for Identification of Structural Dynamic Systems," by O. Maruyama, C-B. Yun, M. Hoshiya and M. Shinozuka, 5/19/89, (PB90-109877/AS).
- NCEER-89-0015 "Response of Frames With Bolted Semi-Rigid Connections, Part I - Experimental Study and Analytical Predictions," by P.J. DiCorso, A.M. Reinhorn, J.R. Dickerson, J.B. Radzinski and W.L. Harper, 6/1/89, to be published.
- NCEER-89-0016 "ARMA Monte Carlo Simulation in Probabilistic Structural Analysis," by P.D. Spanos and M.P. Mignolet, 7/10/89, (PB90-109893/AS).
- NCEER-89-P017 "Preliminary Proceedings from the Conference on Disaster Preparedness - The Place of Earthquake Education in Our Schools," Edited by K.E.K. Ross, 6/23/89.
- NCEER-89-0017 "Proceedings from the Conference on Disaster Preparedness - The Place of Earthquake Education in Our Schools," Edited by K.E.K. Ross, 12/31/89, (PB90-207895). This report is available only through NTIS (see address given above).
- NCEER-89-0018 "Multidimensional Models of Hysteretic Material Behavior for Vibration Analysis of Shape Memory Energy Absorbing Devices, by E.J. Graesser and F.A. Cozzarelli, 6/7/89, (PB90-164146/AS).
- NCEER-89-0019 "Nonlinear Dynamic Analysis of Three-Dimensional Base Isolated Structures (3D-BASIS)," by S. Nagarajaiah, A.M. Reinhorn and M.C. Constantinou, 8/3/89, (PB90-161936/AS). This report is available only through NTIS (see address given above).
- NCEER-89-0020 "Structural Control Considering Time-Rate of Control Forces and Control Rate Constraints," by F.Y. Cheng and C.P. Pantelides, 8/3/89, (PB90-120445/AS).
- NCEER-89-0021 "Subsurface Conditions of Memphis and Shelby County," by K.W. Ng, T-S. Chang and H-H.M. Hwang, 7/26/89, (PB90-120437/AS).
- NCEER-89-0022 "Seismic Wave Propagation Effects on Straight Jointed Buried Pipelines," by K. Elhadi and M.J. O'Rourke, 8/24/89, (PB90-162322/AS).
- NCEER-89-0023 "Workshop on Serviceability Analysis of Water Delivery Systems," edited by M. Grigoriu, 3/6/89, (PB90-127424/AS).
- NCEER-89-0024 "Shaking Table Study of a 1/5 Scale Steel Frame Composed of Tapered Members," by K.C. Chang, J.S. Hwang and G.C. Lee, 9/18/89, (PB90-160169/AS).
- NCEER-89-0025 "DYNA1D: A Computer Program for Nonlinear Seismic Site Response Analysis - Technical Documentation," by Jean H. Prevost, 9/14/89, (PB90-161944/AS). This report is available only through NTIS (see address given above).
- NCEER-89-0026 "1:4 Scale Model Studies of Active Tendon Systems and Active Mass Dampers for Aseismic Protection," by A.M. Reinhorn, T.T. Soong, R.C. Lin, Y.P. Yang, Y. Fukao, H. Abe and M. Nakai, 9/15/89, (PB90-173246/AS).
- NCEER-89-0027 "Scattering of Waves by Inclusions in a Nonhomogeneous Elastic Half Space Solved by Boundary Element Methods," by P.K. Hadley, A. Askar and A.S. Cakmak, 6/15/89, (PB90-145699/AS).
- NCEER-89-0028 "Statistical Evaluation of Deflection Amplification Factors for Reinforced Concrete Structures," by H.H.M. Hwang, J-W. Jaw and A.L. Ch'ng, 8/31/89, (PB90-164633/AS).
- NCEER-89-0029 "Bedrock Accelerations in Memphis Area Due to Large New Madrid Earthquakes," by H.H.M. Hwang, C.H.S. Chen and G. Yu, 11/7/89, (PB90-162330/AS).

- NCEER-89-0030 "Seismic Behavior and Response Sensitivity of Secondary Structural Systems," by Y.Q. Chen and T.T. Soong, 10/23/89, (PB90-164658/AS).
- NCEER-89-0031 "Random Vibration and Reliability Analysis of Primary-Secondary Structural Systems," by Y. Ibrahim, M. Grigoriu and T.T. Soong, 11/10/89, (PB90-161951/AS).
- NCEER-89-0032 "Proceedings from the Second U.S. - Japan Workshop on Liquefaction, Large Ground Deformation and Their Effects on Lifelines, September 26-29, 1989," Edited by T.D. O'Rourke and M. Hamada, 12/1/89, (PB90-209388/AS).
- NCEER-89-0033 "Deterministic Model for Seismic Damage Evaluation of Reinforced Concrete Structures," by J.M. Bracci, A.M. Reinhorn, J.B. Mander and S.K. Kunnath, 9/27/89.
- NCEER-89-0034 "On the Relation Between Local and Global Damage Indices," by E. DiPasquale and A.S. Cakmak, 8/15/89, (PB90-173865).
- NCEER-89-0035 "Cyclic Undrained Behavior of Nonplastic and Low Plasticity Silts," by A.J. Walker and H.E. Stewart, 7/26/89, (PB90-183518/AS).
- NCEER-89-0036 "Liquefaction Potential of Surficial Deposits in the City of Buffalo, New York," by M. Budhu, R. Giese and L. Baumgrass, 1/17/89, (PB90-208455/AS).
- NCEER-89-0037 "A Deterministic Assessment of Effects of Ground Motion Incoherence," by A.S. Veletsos and Y. Tang, 7/15/89, (PB90-164294/AS).
- NCEER-89-0038 "Workshop on Ground Motion Parameters for Seismic Hazard Mapping," July 17-18, 1989, edited by R.V. Whitman, 12/1/89, (PB90-173923/AS).
- NCEER-89-0039 "Seismic Effects on Elevated Transit Lines of the New York City Transit Authority," by C.J. Costantino, C.A. Miller and E. Heymsfield, 12/26/89, (PB90-207887/AS).
- NCEER-89-0040 "Centrifugal Modeling of Dynamic Soil-Structure Interaction," by K. Weissman, Supervised by J.H. Prevost, 5/10/89, (PB90-207879/AS).
- NCEER-89-0041 "Linearized Identification of Buildings With Cores for Seismic Vulnerability Assessment," by I-K. Ho and A.E. Aktan, 11/1/89, (PB90-251943/AS).
- NCEER-90-0001 "Geotechnical and Lifeline Aspects of the October 17, 1989 Loma Prieta Earthquake in San Francisco," by T.D. O'Rourke, H.E. Stewart, F.T. Blackburn and T.S. Dickerman, 1/90, (PB90-208596/AS).
- NCEER-90-0002 "Nonnormal Secondary Response Due to Yielding in a Primary Structure," by D.C.K. Chen and L.D. Lutes, 2/28/90, (PB90-251976/AS).
- NCEER-90-0003 "Earthquake Education Materials for Grades K-12," by K.E.K. Ross, 4/16/90, (PB91-113415/AS).
- NCEER-90-0004 "Catalog of Strong Motion Stations in Eastern North America," by R.W. Busby, 4/3/90, (PB90-251984/AS).
- NCEER-90-0005 "NCEER Strong-Motion Data Base: A User Manual for the GeoBase Release (Version 1.0 for the Sun3)," by P. Friberg and K. Jacob, 3/31/90 (PB90-258062/AS).
- NCEER-90-0006 "Seismic Hazard Along a Crude Oil Pipeline in the Event of an 1811-1812 Type New Madrid Earthquake," by H.H.M. Hwang and C-H.S. Chen, 4/16/90(PB90-258054).
- NCEER-90-0007 "Site-Specific Response Spectra for Memphis Sheahan Pumping Station," by H.H.M. Hwang and C.S. Lee, 5/15/90, (PB91-108811/AS).

- NCEER-90-0008 "Pilot Study on Seismic Vulnerability of Crude Oil Transmission Systems," by T. Ariman, R. Dobry, M. Grigoriu, F. Kozin, M. O'Rourke, T. O'Rourke and M. Shinozuka, 5/25/90, (PB91-108837/AS).
- NCEER-90-0009 "A Program to Generate Site Dependent Time Histories: EQGEN," by G.W. Ellis, M. Srinivasan and A.S. Cakmak, 1/30/90, (PB91-108829/AS).
- NCEER-90-0010 "Active Isolation for Seismic Protection of Operating Rooms," by M.E. Talbott, Supervised by M. Shinozuka, 6/8/9, (PB91-110205/AS).
- NCEER-90-0011 "Program LINEARID for Identification of Linear Structural Dynamic Systems," by C-B. Yun and M. Shinozuka, 6/25/90, (PB91-110312/AS).
- NCEER-90-0012 "Two-Dimensional Two-Phase Elasto-Plastic Seismic Response of Earth Dams," by A.N. Yiagos, Supervised by J.H. Prevost, 6/20/90, (PB91-110197/AS).
- NCEER-90-0013 "Secondary Systems in Base-Isolated Structures: Experimental Investigation, Stochastic Response and Stochastic Sensitivity," by G.D. Manolis, G. Juhn, M.C. Constantinou and A.M. Reinhorn, 7/1/90, (PB91-110320/AS).
- NCEER-90-0014 "Seismic Behavior of Lightly-Reinforced Concrete Column and Beam-Column Joint Details," by S.P. Pessiki, C.H. Conley, P. Gergely and R.N. White, 8/22/90, (PB91-108795/AS).
- NCEER-90-0015 "Two Hybrid Control Systems for Building Structures Under Strong Earthquakes," by J.N. Yang and A. Danielians, 6/29/90, (PB91-125393/AS).
- NCEER-90-0016 "Instantaneous Optimal Control with Acceleration and Velocity Feedback," by J.N. Yang and Z. Li, 6/29/90, (PB91-125401/AS).
- NCEER-90-0017 "Reconnaissance Report on the Northern Iran Earthquake of June 21, 1990," by M. Mehrain, 10/4/90, (PB91-125377/AS).
- NCEER-90-0018 "Evaluation of Liquefaction Potential in Memphis and Shelby County," by T.S. Chang, P.S. Tang, C.S. Lee and H. Hwang, 8/10/90, (PB91-125427/AS).
- NCEER-90-0019 "Experimental and Analytical Study of a Combined Sliding Disc Bearing and Helical Steel Spring Isolation System," by M.C. Constantinou, A.S. Mokha and A.M. Reinhorn, 10/4/90, (PB91-125385/AS).
- NCEER-90-0020 "Experimental Study and Analytical Prediction of Earthquake Response of a Sliding Isolation System with a Spherical Surface," by A.S. Mokha, M.C. Constantinou and A.M. Reinhorn, 10/11/90, (PB91-125419/AS).
- NCEER-90-0021 "Dynamic Interaction Factors for Floating Pile Groups," by G. Gazetas, K. Fan, A. Kaynia and E. Kausel, 9/10/90, (PB91-170381/AS).
- NCEER-90-0022 "Evaluation of Seismic Damage Indices for Reinforced Concrete Structures," by S. Rodriguez-Gomez and A.S. Cakmak, 9/30/90, PB91-171322/AS).
- NCEER-90-0023 "Study of Site Response at a Selected Memphis Site," by H. Desai, S. Ahmad, E.S. Gazetas and M.R. Oh, 10/11/90, (PB91-196857/AS).
- NCEER-90-0024 "A User's Guide to Strongmo: Version 1.0 of NCEER's Strong-Motion Data Access Tool for PCs and Terminals," by P.A. Friberg and C.A.T. Susch, 11/15/90, (PB91-171272/AS).
- NCEER-90-0025 "A Three-Dimensional Analytical Study of Spatial Variability of Seismic Ground Motions," by L-L. Hong and A.H.-S. Ang, 10/30/90, (PB91-170399/AS).

- NCEER-90-0026 "MUMOID User's Guide - A Program for the Identification of Modal Parameters," by S. Rodriguez-Gomez and E. DiPasquale, 9/30/90, (PB91-171298/AS).
- NCEER-90-0027 "SARCF-II User's Guide - Seismic Analysis of Reinforced Concrete Frames," by S. Rodriguez-Gomez, Y.S. Chung and C. Meyer, 9/30/90, (PB91-171280/AS).
- NCEER-90-0028 "Viscous Dampers: Testing, Modeling and Application in Vibration and Seismic Isolation," by N. Makris and M.C. Constantinou, 12/20/90 (PB91-190561/AS).
- NCEER-90-0029 "Soil Effects on Earthquake Ground Motions in the Memphis Area," by H. Hwang, C.S. Lee, K.W. Ng and T.S. Chang, 8/2/90, (PB91-190751/AS).
- NCEER-91-0001 "Proceedings from the Third Japan-U.S. Workshop on Earthquake Resistant Design of Lifeline Facilities and Countermeasures for Soil Liquefaction, December 17-19, 1990," edited by T.D. O'Rourke and M. Hamada, 2/1/91, (PB91-179259/AS).
- NCEER-91-0002 "Physical Space Solutions of Non-Proportionally Damped Systems," by M. Tong, Z. Liang and G.C. Lee, 1/15/91, (PB91-179242/AS).
- NCEER-91-0003 "Seismic Response of Single Piles and Pile Groups," by K. Fan and G. Gazetas, 1/10/91, (PB92-174994/AS)..
- NCEER-91-0004 "Damping of Structures: Part 1 - Theory of Complex Damping," by Z. Liang and G. Lee, 10/10/91, (PB92-197235/AS).
- NCEER-91-0005 "3D-BASIS - Nonlinear Dynamic Analysis of Three Dimensional Base Isolated Structures: Part II," by S. Nagarajaiah, A.M. Reinhorn and M.C. Constantinou, 2/28/91, (PB91-190553/AS).
- NCEER-91-0006 "A Multidimensional Hysteretic Model for Plasticity Deforming Metals in Energy Absorbing Devices," by E.J. Graesser and F.A. Cozzarelli, 4/9/91.
- NCEER-91-0007 "A Framework for Customizable Knowledge-Based Expert Systems with an Application to a KBES for Evaluating the Seismic Resistance of Existing Buildings," by E.G. Ibarra-Anaya and S.J. Fenves, 4/9/91, (PB91-210930/AS).
- NCEER-91-0008 "Nonlinear Analysis of Steel Frames with Semi-Rigid Connections Using the Capacity Spectrum Method," by G.G. Deierlein, S-H. Hsieh, Y-J. Shen and J.F. Abel, 7/2/91, (PB92-113828/AS).
- NCEER-91-0009 "Earthquake Education Materials for Grades K-12," by K.E.K. Ross, 4/30/91, (PB91-212142/AS).
- NCEER-91-0010 "Phase Wave Velocities and Displacement Phase Differences in a Harmonically Oscillating Pile," by N. Makris and G. Gazetas, 7/8/91, (PB92-108356/AS).
- NCEER-91-0011 "Dynamic Characteristics of a Full-Size Five-Story Steel Structure and a 2/5 Scale Model," by K.C. Chang, G.C. Yao, G.C. Lee, D.S. Hao and Y.C. Yeh," 7/2/91.
- NCEER-91-0012 "Seismic Response of a 2/5 Scale Steel Structure with Added Viscoelastic Dampers," by K.C. Chang, T.T. Soong, S-T. Oh and M.L. Lai, 5/17/91 (PB92-110816/AS).
- NCEER-91-0013 "Earthquake Response of Retaining Walls; Full-Scale Testing and Computational Modeling," by S. Alampalli and A-W.M. Elgamal, 6/20/91, to be published.
- NCEER-91-0014 "3D-BASIS-M: Nonlinear Dynamic Analysis of Multiple Building Base Isolated Structures," by P.C. Tsopelas, S. Nagarajaiah, M.C. Constantinou and A.M. Reinhorn, 5/28/91, (PB92-113885/AS).

- NCEER-91-0015 "Evaluation of SEAOC Design Requirements for Sliding Isolated Structures," by D. Theodossiou and M.C. Constantinou, 6/10/91, (PB92-114602/AS).
- NCEER-91-0016 "Closed-Loop Modal Testing of a 27-Story Reinforced Concrete Flat Plate-Core Building," by H.R. Somaprasad, T. Toksoy, H. Yoshiyuki and A.E. Aktan, 7/15/91, (PB92-129980/AS).
- NCEER-91-0017 "Shake Table Test of a 1/6 Scale Two-Story Lightly Reinforced Concrete Building," by A.G. El-Attar, R.N. White and P. Gergely, 2/28/91.
- NCEER-91-0018 "Shake Table Test of a 1/8 Scale Three-Story Lightly Reinforced Concrete Building," by A.G. El-Attar, R.N. White and P. Gergely, 2/28/91.
- NCEER-91-0019 "Transfer Functions for Rigid Rectangular Foundations," by A.S. Veletsos, A.M. Prasad and W.H. Wu, 7/31/91, to be published.
- NCEER-91-0020 "Hybrid Control of Seismic-Excited Nonlinear and Inelastic Structural Systems," by J.N. Yang, Z. Li and A. Danielians, 8/1/91.
- NCEER-91-0021 "The NCEER-91 Earthquake Catalog: Improved Intensity-Based Magnitudes and Recurrence Relations for U.S. Earthquakes East of New Madrid," by L. Seeber and J.G. Armbruster, 8/28/91, (PB92-176742/AS).
- NCEER-91-0022 "Proceedings from the Implementation of Earthquake Planning and Education in Schools: The Need for Change - The Roles of the Changemakers," by K.E.K. Ross and F. Winslow, 7/23/91, (PB92-129998/AS).
- NCEER-91-0023 "A Study of Reliability-Based Criteria for Seismic Design of Reinforced Concrete Frame Buildings," by H.H.M. Hwang and H-M. Hsu, 8/10/91.
- NCEER-91-0024 "Experimental Verification of a Number of Structural System Identification Algorithms," by R.G. Ghanem, H. Gavin and M. Shinozuka, 9/18/91, (PB92-176577/AS).
- NCEER-91-0025 "Probabilistic Evaluation of Liquefaction Potential," by H.H.M. Hwang and C.S. Lee," 11/25/91.
- NCEER-91-0026 "Instantaneous Optimal Control for Linear, Nonlinear and Hysteretic Structures - Stable Controllers," by J.N. Yang and Z. Li, 11/15/91, (PB92-163807/AS).
- NCEER-91-0027 "Experimental and Theoretical Study of a Sliding Isolation System for Bridges," by M.C. Constantinou, A. Kartoum, A.M. Reinhorn and P. Bradford, 11/15/91, (PB92-176973/AS).
- NCEER-92-0001 "Case Studies of Liquefaction and Lifeline Performance During Past Earthquakes, Volume 1: Japanese Case Studies," Edited by M. Hamada and T. O'Rourke, 2/17/92, (PB92-197243/AS).
- NCEER-92-0002 "Case Studies of Liquefaction and Lifeline Performance During Past Earthquakes, Volume 2: United States Case Studies," Edited by T. O'Rourke and M. Hamada, 2/17/92, (PB92-197250/AS).
- NCEER-92-0003 "Issues in Earthquake Education," Edited by K. Ross, 2/3/92.
- NCEER-92-0004 "Proceedings from the First U.S. - Japan Workshop on Earthquake Protective Systems for Bridges," 2/4/92, to be published.
- NCEER-92-0005 "Seismic Ground Motion from a Haskell-Type Source in a Multiple-Layered Half-Space," A.P. Theoharis, G. Deodatis and M. Shinozuka, 1/2/92, to be published.
- NCEER-92-0006 "Proceedings from the Site Effects Workshop," Edited by R. Whitman, 2/29/92, (PB92-197201/AS).

- NCEER-92-0007 "Engineering Evaluation of Permanent Ground Deformations Due to Seismically-Induced Liquefaction," by M.H. Baziar, R. Dobry and A-W.M. Elgamal, 3/24/92.
- NCEER-92-0008 "A Procedure for the Seismic Evaluation of Buildings in the Central and Eastern United States," by C.D. Poland and J.O. Malley, 4/2/92.
- NCEER-92-0009 "Experimental and Analytical Study of a Hybrid Isolation System Using Friction Controllable Sliding Bearings," by Q. Feng, S. Fujii and M. Shinozuka, 2/15/92, to be published.
- NCEER-92-0010 "Seismic Resistance of Slab-Column Connections in Existing Non-Ductile Flat-Plate Buildings," by A.J. Durrani and Y. Du, 5/18/92.
- NCEER-92-0011 "The Hysteretic and Dynamic Behavior of Brick Masonry Walls Upgraded by Ferrocement Coatings Under Cyclic Loading and Strong Simulated Ground Motion," by H. Lee and S.P. Prawel, 5/11/92, to be published.
- NCEER-92-0012 "Study of Wire Rope Systems for Seismic Protection of Equipment in Buildings," by G.F. Demetriades, M.C. Constantinou and A.M. Reinhorn, 5/20/92.
- NCEER-92-0013 "Shape Memory Structural Dampers: Material Properties, Design and Seismic Testing," by P.R. Witting and F.A. Cozzarelli, 5/26/92.
- NCEER-92-0014 "Longitudinal Permanent Ground Deformation Effects on Buried Continuous Pipelines," by M.J. O'Rourke, and C. Nordberg, 6/15/92.
- NCEER-92-0015 "A Simulation Method for Stationary Gaussian Random Functions Based on the Sampling Theorem," by M. Grigoriu and S. Balopoulou, 6/11/92.

